ADDIS ABABA UNIVERSITY

SCHOOL OF GRADUATE STUDIES

ADDIS ABABA INSTITUTE OF TECHNOLOGY

ELECTRICAL AND COMPUTER ENGINEERING DEPARTMENT

Modeling and Control of a Quad-rotor Unmanned Aerial Vehicle at Hovering Position

By

Ruth Tesfaye

Advisor

Ato Lebsework Negash

A Thesis Submitted to the School of Graduate Studies of Addis Ababa University in Partial Fulfillment of the Requirements for the Degree of Masters of Science in Electrical Engineering

December, 2012

Addis Ababa, Ethiopia

Abstract

This thesis titled Modeling and Control of a Quad-rotor Unmanned Aerial vehicle at hovering Position by Ruth Tesfaye presents the study of modeling and control of quad-rotor Unmanned Aerial vehicle (UAV) characteristics that could be used for any of its application.

Quad-rotor UAVs consist of two pairs of counter rotating rotors placed at the end of a cross configuration; symmetrical body about the center of gravity that coincides with the origin of the body frame of reference. The Newton-Euler formulation has been used to derive the defining equations of motion of the system at hovering position i.e. the six degree-of-freedom. Based on the verified model, control strategies were developed using linear PID controller and an LQR controller. The PID controller was adopted as a reference control law from the work of A.ouladi [1].

A numerical simulation was then conducted using MATLAB® Simulink®. First, the derived model was simulated to verify the behavior of the quad-rotor for model verification, and then a second simulation was conducted to determine the effectiveness of the developed control law. The results and the interpretations of this study are then presented and discussed on their respective areas.

Key words: Quad-rotor, PID controller, LQR controller, Hovering position, equilibrium Point

Table of Contents

Abstract i
Table of Contents ii
List of Tables iv
List of Figures iv
List of Acronyms v
1 Introduction 1
1.1 Background 1
1.2 Literature Review 2
1.3 Statement of the Problem 4
1.4 Objective 4
1.5 Methodology 5
1.6 Scope 5
1.7 Thesis Outline 6
2 Overview of Unmanned Aerial Vehicle 7
2.1 Unmanned Aerial Vehicles (UAVs) 9
2.2 Quad-rotor 10
2.2.1 Background on Quad-rotor 10
2.2.2 Research on Quad-rotors 12
3 Modeling and Simulation 15
3.1 Common Conventions 16
3.1.1 Frames of Reference 16
3.1.2 Rotation Matrix 18
3.1.3 Transfer Matrix 18
3.1.4 Assumptions 19
3.2 Basic forces 19
3.3 Physical Effects 20
3.4 Flight Conditions 21
3.5 Quad-rotor Dynamics 22
3.5.1 Principle of Operation 22
3.5.2 Equations of motion 28
3.6 Model Verification 35

4 Controller Design and Results 46
4.1 PID Controller 46
4.2 LQR Controller 49
4.2.1 Design using Pole Placement 50
4.2.2 Design LQ-Servo feedback using LQR technique 52
4.3 Disturbances Introduced 55
5 Conclusions and Recommendations 66
5.1 Contribution 66
5.2 Conclusion 66
5.3 Future Works 68
6 References 69
Appendix 71
A. Rotation Matrix 71
B. Transfer Matrix 73
C. Parameters of DraganFlyer IV 74
D. Details on Linearization 74

List of Tables

Table 1-1: Methodology followed for this thesis 5
Table 2-1: State of the Art Quad-rotors 13

List of Figures

Figure 2-1: Chinese Bamboo Dragon Fly Prototype 7
Figure 2-2: Launoy and Bienvenu's model in 1783 8
Figure 2-3: Sir George Cayley's first manned glider 8
Figure 2-4: The Breguet-Richet Gyroplane No.1-Quad-rotor of 1907 11
Figure 2-5: The De Bothezat Flying Octopus of 1923 and Oemichen's quad-rotor of 1924 11
Figure 3-1: Steps followed in creating the model 16
Figure 3-2: Inertial and Body Fixed Frame 17
Figure 3-3: Ilustration about Thrust/Lift force 20
Figure 3-4: Conceptual Diagram of a Quad-rotor 23
Figure 3-5: Thrust 24
Figure 3-6: Roll 25
Figure 3-7: Pitch 26
Figure 3-8: Yaw 27
Figure 3-9: Ascend (top), Descend (bottom) 28
Figure 3-10: Generic State space model 34
Figure 3-11: Model as built in Simulink 35
Figure 3-12: Quad-rotor descending 38
Figure 3-13: Quad-rotor Ascending 39
Figure 3-14: Quad-rotor Hovering at zero equilibrium point 40
Figure 3-15: Quad-rotor Rolling to the right 41
Figure 3-16: Force decomposition showing φ and Y drfit are coupled 41
Figure 3-17: Quad-rotorpitching to forward 43
Figure 3-18: Force decomposition showing that θ and X drift are coupled 43
Figure 3-19: Quad-rotor yawing to the clockwiseand hovering still at 8m 45
Figure 4-1: PID controller concept implemented in this work 47
Figure 4-2: PID Controller block 48
Figure 4-3: Stabilization of Altitude using a PID controller 48
Figure 4-4: Stabilization of Euler Angles using PID controller 49
Figure 4-5: State feedback /General LQR (u=-kx)/ 50
Figure 4-6:LQR controller using pole placement in Simulink 51
Figure 4-7: Translational motion using pole placement Technique 51
Figure 4-8:Rotational motion using pole placement Technique 52
Figure 4-9:LQ-Servo feedback using LQR technique Simulink block 54
Figure 4-10: Translational motion using LQ-servo feedback technique 54

Figure 4-11: Rotational motion using LQ-Servo feedback technique 55
Figure 4-12:Conceptual Diagram showing the craft in a windy environment............................. 56
Figure 4-13: Disturbance model 57
Figure 4-14: Altitude and Attitude Stabilization with disturbance using PID controller 58
Figure 4-15:Position stabilization after disturbance using LQR controller 59
Figure 4-16: Attitude Stabilization with disturbance using LQR controller................................ 60
Figure 4-17:Side Jerk to the X-axis and Z-axis 61
Figure 4-18:Side Jerk Disturbance model.. 62
Figure 4-19:Altitude and Attitude Stabilization with Jerking force to the Z-axis using PID controller 63
Figure 4-20: Position Stabilization with Side jerk to the X-axis using LQR controller 64
Figure 4-21: Attitude Stabilization with Side jerk to the X-axis using LQR controller 65

List of Acronyms

ARE	Algebraic Riccati Equation
BFF	Body Fixed Frame
CoG	Center of Gravity
CCW	Counter Clock wise
CW	Clock wise
DoF	Degree of Freedom
IF	Inertial Frame
LQR	Linear Quadratic Regulator
PID	Proportional, Integrator and Derivative
SISO	Single Input Single Output
UAV	Unmanned Aerial Vehicle
VTOL	Vertical Take Off and Landing

1 Introduction

This chapter provides a general overview on the background, goal, methodology and the layout of the thesis.

1.1 Background

The need of robots replacing humans in precarious and inaccessible areas has been the spot of interest for many researches in different industries; one of these interesting research areas is the Unmanned Aerial Vehicle (UAV). They have been studied and implemented for different applications so far, such as power line fault detection, surveillance, reconnaissance, target acquisition, agricultural spraying etc. [2]

UAVs have two main types of configurations, i.e. fixed wing UAV and rotor craft UAV. The fixed wing aircrafts travel long range and are capable of flying at high altitude but lack maneuverability vital for UAVs. On the other hand, rotorcrafts have advantages such as maneuverability capabilities; hovering over targets, taking off and landing in limited spaces as compared to fixed wing vehicles which have a conventional type of taking off and landing requiring a runway. [3]

In this thesis, a quad-rotor which is classified as a rotorcraft is studied. It is an aircraft lifted and propelled by four rotors. It uses fixed-pitch blades, whose rotor pitch does not vary as the blades rotate. Control of motion of a quad-rotor can be achieved by varying the relative speed of each rotor to change the thrust and torque produced by each. Quad-rotor from the rotorcraft category is chosen for some of the applications mentioned above due to its simplicity in construction, ease of maintenance and an uncomplicated dynamics compared to a standard helicopter using a main and tail rotor. [4]

1.2 Literature Review

Different literatures have approached the research of quad-rotor UAV in different ways and some of them are discussed here below briefly.

In the paper by Hugo Meric [5], Newton-Euler and also the Lagrange-Euler equations were used for modeling the translational and rotational equations of motion respectively. Attitude and altitude stabilization has been achieved using four independent PD controllers while a reinforcement learning controlling algorithm has been used for comparison for the altitude controller. Despite having the advantage of easier implementation and better settling time the PD controllers did not have better stability results compared to the latter controller.

A.Ouladi, [1], formulated the equations of motion that govern the dynamics of the craft mathematically using the Newton-Euler mechanics. PID controller has been used to stabilize the yaw angle and the altitude on a square wave trajectory. It is recommended that the other DoF determining its position in space be also stabilized for a better outcome in controlling the motion of the craft.

In the literature by Yoon [6] , it has been already exhibited that the craft is capable to fly with a PID controller; model has been established using the Euler-Lagrange equations and validated. The validation in hover mode was satisfactory for designing an optimal control such as LQR. This controller has been used to stabilize the attitude for near stationary flight. Recommendations are to include an altitude controller and to have knowledge of its space orientation (i.e. position controller).

S.Bouabdallah, A.Noth and R.Siegwart, [7] , have used the Newton Euler formulation for modeling. PID and LQR controllers have been compared for stabilizing the attitude of the UAV. The latter controller has a better performance but takes a long time to settle. Future work is to enhance the autonomous flight by including the stability of position.

In the work by Birkan Tunc, [8], the mathematical model was generally deduced from the Newton-Euler mechanism. Fuzzy logic was used as control mechanism and first of the angular subsystem was stabilized using 3 independent fuzzy logic controllers while the altitude was controlled with the realization of the control input using fuzzy logic controller. The three independent Fuzzy Logic Controllers are setup with 9 rules. Increasing rules increases the computation time hence, minimum number of rules is used. To control a quad-rotor UAV successfully outdoor one has to consider the disturbances which arise from the atmospheric conditions such as wind gusts this could be taken as an input for future work.

The work by M.Raju Hossain, [9], presents a dynamic model of such a vehicle using bond graphs. The bond graph that is produced here follows the Newton-Euler formalism which has been widely used for modeling this kind of helicopter. Initially to explore the performance of the model, open loop simulation was performed. The simulation demonstrates the flight maneuver which satisfies the theoretical trajectories that the quad-rotor is supposed to perform at certain combinations of the rotor thrust. Possible extensions to the controller might involve control of its position or co-ordinates in space that may lead the model to be even more accurate and practical.

Tommaso Bresciani, [10], also derived the mathematical model of the quad-rotor using the Newton Euler Formulation. Two levels of controller were implemented i.e. the low level controller and the high level controller. The low level controller’s goal was the stabilization of the height and attitude whereas the high level controller is cascaded with the previous controller to follow for position requirements. Other tasks, computed by the high level controller, can be obstacle avoidance and trajectory planning. For future aerodynamic effects could be considered for stabilization during a non-hovering operation.

1.3 Statement of the Problem

Different papers have recommendations for future work for the quad-rotor configuration UAV. Recommendations from the literatures mentioned in the previous section, shall suffice as a ground breaking for the work to be carried out in this thesis. The controller algorithms to be used in this work are from the above mentioned literatures and will carry out to achieve the performances that have been recommended.

So the main work of this thesis is to overcome some of the inadequacies or accomplish the recommendations; these are lack of environment disturbances [8], lack of knowledge of its position in space [9], [1], [6], [7] and lack of adaptability for the case of non-hovering operation [10].

Hence, this work will be looking into the following two recommendations these are the lack of environmental disturbances and lack of knowledge of its position in space by the use of an appropriate modeling technique with an appropriate controller.

1.4 Objective

General Objective

- Understanding the dynamics of a quad-rotor
- Choose a comprehensible modeling technique
- Design a controller to stabilize the craft at hovering position.
- Design a controller to stabilize the craft at hovering position after disturbances have been introduced.

Specific Objective

- Linearize the model to a hovering equilibrium point

- Simulate model with MATLAB-Simulink for verification
- Design Controller based on the linearized model
- Introduce disturbances and stabilize craft back to hovering position

1.5 Methodology

Table 1-1: Methodology followed for this thesis

Methodology	Tasks (in Detail)
Literature View	Reading books, articles, forums, simulation tools related to the subject matter
System Modeling	Formulating the mathematical relation of the dynamics (motion) of the quad-rotor.
Controller Design	Designing an appropriate controller based on the model formulated.
Simulation	Simulation of the modeled dynamics and controller using MATLAB -Simulink
Analysis and Interpretation	Analysis and interpretation of the result
Performance Comparison	Compare results between different control algorithms

1.6 Scope

In this work the dynamics of quad-rotor shall be studied and a mathematical model will be formulated using the Newton-Euler formalism; based on the model a control law will be designed to stabilize the craft at hovering position. PID controller is chosen as a benchmark control algorithm which is adapted from the literature [1] where later it will be used for comparison of performance.

The parameter of the quad-rotor for simulation is adopted from a literature that uses a commercially available radio controlled craft called Draganflyer X4 manufactured by Dragaflyer Innovations Inc. [11] Included in Appendix C

The outcome of this research shall be based on the simulation of the proposed techniques using a simulation tool (MATLAB or any other that is available).

1.7 Thesis Outline

Chapter 2 deals with an overview and essential concepts about flight, unmanned aerial vehicles with depth about quad-rotor and a summary about state of the art quad-rotors researched recently.

Chapter 3 discusses about common terminologies and conventions used at the beginning of the modeling phase. The model (equations of motion) is derived by using the Newton-Euler formalism and finally verification of the model is shown in the MATLAB-Simulink environment.

Chapter 4 presents the control law designed to stabilize the UAV at hovering position by using PID and LQR controller.

Chapter 5 provides the conclusion drawn and recommendations for future work.

References used in this work are presented in numerical order; additional concepts and some other materials that are relevant to this work are included in appendix.

2 Overview of Unmanned Aerial Vehicle

This chapter provides a general overview about how flying started. It discusses about general points on UAVs, background on quad-rotors and the recent state of the art versions of the rotorcraft.

"The idea of a vehicle that could lift itself vertically from the ground and hover motionless in the air was probably born at the same time that man first dreamed of flying." Igor Ivanovitch Sikorsky [12]. With this dream man has reached to the summit of different types of aircrafts.

Aircrafts are vehicles that fly by gaining support from the air. Broadly, they are classified as manned aircraft (onboard pilot) and unmanned aircraft (aerial vehicles that may be remotely controlled or self-controlled); might also be classified by different criteria such as lift type, propulsion, usage and others. Lift involving wings is common to fixed-wing aircrafts and for rotorcrafts wing shaped rotors are spun. [13]

Vertical Takeoff and Landing (VTOL) is a type of lift where rotorcrafts are classified to; this emerged from Chinese toys (top) which were the first form of man-made flying objects invented around 500 BC in China. Succeeding the tops kites were the earliest known record of flight around 200 BC in China when a General flew over enemy territory to calculate the length of tunnel required to enter the region. [13]

Figure 2-1: Chinese Bamboo Dragon Fly Prototype

The earliest versions of the Chinese top consisted of feathers or bamboo (horizontal bar) at the end of a stick, which was rapidly spun between the hands to generate lift and then released into free flight Figure 2-1. Observations and Fascinations of Chinese tops have led a pioneering development to the world of flights and aircrafts. Figure 2-2 shows a coaxial version of the Chinese top in a model consisting of a counter rotating set of turkey feathers created by the French naturalist Launoy and Bienvenu in 1783. [13]

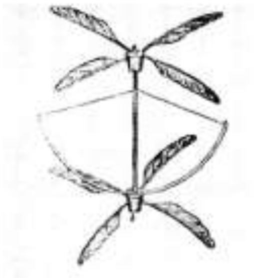

Figure 2-2: Launoy and Bienvenu's model in 1783

Sir George Cayley's*"Father of Aviation"* fascination with flight of the Chinese top led him to design and construct a whirling-arm device in 1804, which was probably one of the first scientific attempts to study the aerodynamic forces produced by lifting wings. The first heavier-than-air craft capable of controlled free-flight were gliders Figure 2-3. A glider designed by Cayley carried out the first true manned, controlled flight in 1853. [14]

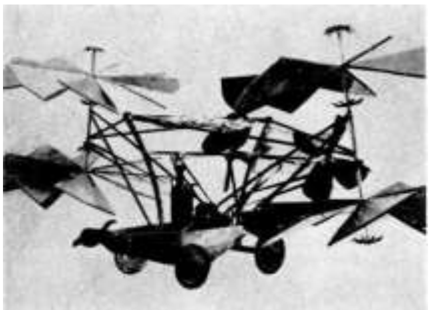

Figure 2-3: Sir George Cayley's first manned glider

Within the last sixty years, rotorcrafts have come a long way emerging from unstable, vibrating contraptions to be capable of VTOL, hover, fly foreword, backward and sideways performing desirable maneuvers. Its civilian roles encompass air ambulance, sea and mountain rescue, crop dusting, firefighting, police surveillance, corporate services, and oil-rig servicing. Military roles of the helicopter are troop transport, mine-sweeping, battlefield surveillance, assault, anti-tank missions and also used in various air-ground and air-sea rescue operations. [12]

2.1 *Unmanned Aerial Vehicles (UAVs)*

According to the free dictionary UAV is defined as "powered, aerial vehicle that does not carry a human operator, uses aerodynamic forces to provide vehicle lift, can fly autonomously or be piloted remotely, can be expendable or recoverable, and can carry a lethal or non-lethal payload."

UAVs come in two varieties: [15]

- Controlled from a remote location (which may even be many thousands of kilometers away, on another continent)
- Fly autonomously based on pre-programmed flight plans using more complex dynamic automation systems.

UAVs have two main types of configurations i.e. fixed wing UAV and rotary wing UAV. The fixed wing aircrafts travel long range and are capable of flying at high altitude but lack maneuverability vital for UAVs, whereas rotorcrafts have simple dynamics and maneuverability capabilities.

Rotorcrafts have the advantage of maneuverability, hovering over targets, taking off and landing in limited spaces as compared to fixed wing vehicles which have a conventional type of taking off and landing requiring a runway.

UAVs are largely applied in the military sector. They perform reconnaissance as well as attack missions; also used in a small but growing number of civil applications, such as firefighting or nonmilitary security work, such as surveillance of pipelines, power line inspection.

UAVs fall into one of six functional categories: [15]

- **Target and decoy** – providing ground and aerial gunnery a target that simulates an enemy aircraft or missile
- **Reconnaissance** – providing battlefield intelligence
- **Combat** – providing attack capability for high-risk missions
- **Logistics** –designed for cargo and logistics operation
- **Research and development** – used to further develop UAV technologies to be integrated into field deployed UAV aircraft
- **Civil and Commercial** –specifically designed for commercial aerial surveillance, search and rescue, oil, gas and mineral exploration and production, transport of goods

2.2 *Quad-rotor*

A recent platform that UAVs have been more in action is the quad-rotor. It has been in the picture ever since 1907 with the invention of the Breguet brothers which is looked over in the next sub-section.

2.2.1 Background on Quad-rotor

French scientist and academician Charles Richet built a small unpiloted helicopter at the beginning of the 20th century. Albeit the failure of the machine; it inspired one of his students who later conducted helicopter experiments with his brother under the guidance of Professor Richet. [14]

In 1907, the Breguet Brothers; Louis and Jacques Breguet built their first human carrying helicopter; they called it the Breguet-Richet Gyroplane No.1, which was a quad-rotor shown in Figure 2-4. Clearly they approached the problem of the helicopter more scientifically than others and thought hard about a configuration that most likely would succeed. It consisted of four long girders made of welded steel tubes and arranged in the form of a horizontal cross. Each rotor consisted of four light, fabric covered biplane type blades, giving a total of

32 separate lifting surfaces. The rotors were placed at each of the four corners of the cross. Diagonally opposite pairs of rotors rotated in opposite directions, thereby canceling torque reaction on the airframe. [14]

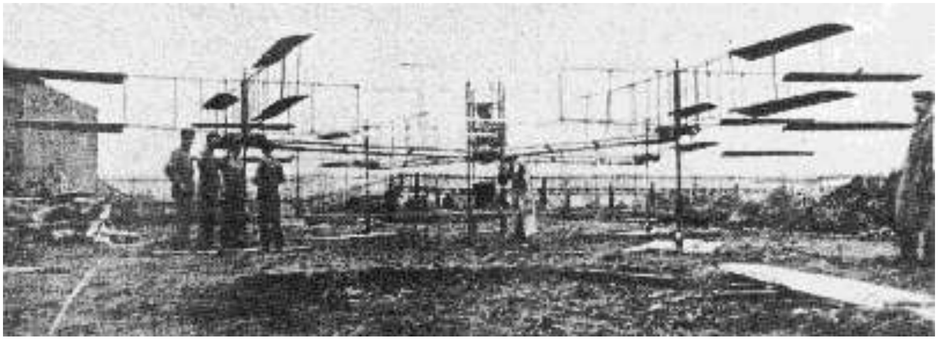

Figure 2-4: The Breguet-Richet Gyroplane No.1-Quad-rotor of 1907

After the Breguet brothers, George de Bothezat built an experimental quad-rotor helicopter shown in Figure 2-5; for the United States Army Air Service in the early 1920s which was also known as the de Bothezat helicopter. Even though its massive six-bladed rotors allowed the craft to successfully fly, it suffered from complexity, control difficulties, and high pilot workload, and was reportedly only capable of forwards flight in a favorable wind. The Army canceled the program in 1924, and the aircraft was scrapped. [13]

Etienne Oemichen's design was successful enough that it became the first rotorcraft to complete 1 km closed circuit flight having the four main rotors featuring five additional rotors for lateral stability Figure 2-5. [14]

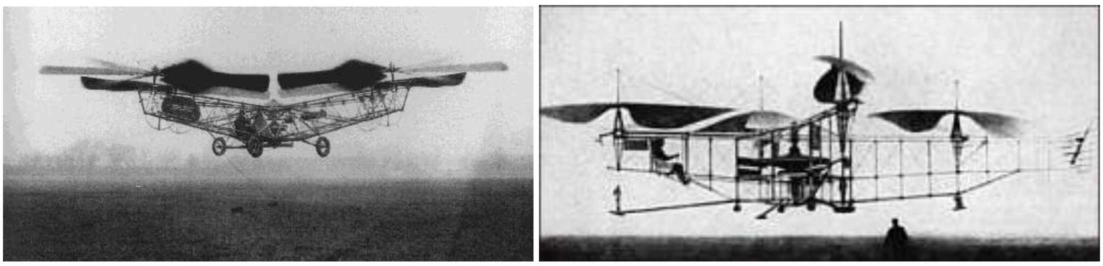

Figure 2-5: The De Bothezat Flying Octopus of 1923 and Oemichen's quad-rotor of 1924

Quad-rotors thus far mentioned are classified as the first generation quad-rotors which were designed to carry one or more passengers where the recent generations are commonly designed to be UAVs and their research begun in early 21st century. [13]

2.2.2 Research on Quad-rotors

Within the last decade universities, students and researchers have inclined their interest in quad-rotor configuration for design and control projects of UAVs. Most of these projects were initiated by hobbyists on commercially available radio controlled toys.

In most cases of researched quad-rotor configuration UAVs the procedure of reaching to the outcome is more or less the same i.e. a modeling technique is selected to define the system mathematically and then a control law is designed. Various modeling techniques and control laws are used on different literatures; and one mathematical modeling technique is chosen based on the technique chosen or matter of the subject studied, finally based on the model the appropriate control is applied.

Some of the modeling techniques and control law used in different projects, researches and their outcome for quad-rotor configuration is described in Table 2-1.

Modeling technique and Control law used for this work are discussed in chapter 3 and chapter 4 respectively.

Table 2-1: State of the Art Quad-rotors

Project Name	Institution	Project (in picture)	Remarks
DraganFlyer Humming Bird	Commercial		Dragan Innovations Inc. [11] Ascending Technologies GmbH [16]
STARMAC	Stanford University		• Independent PD controller for the directly actuated DoF • Linearized equations of motion to develop control laws for waypoint tracking paths. [17]
Quad-rotor	University of Alberta University of Calgary		• Dynamics has been expressed using Newton-Euler Formulation • Cerebellar Model Articulation Controller (Neural Network) • Position and angles are stabilized [18]
OS4	ETH Zurich, Switzerland		• Newton-Euler Formalism for modeling • Integral Backstepping control • Autonomous takeoff and landing has been achieved [19]

Project Name	Institution	Project (in picture)	Remarks
X4 Flyer Mark II	Australia National University		• Large quad-rotor platform with flapping blades • Attitude dynamics was used for tuning the mechanical design • Successfully regulates attitude at low rotor speeds. [20]
			• Adopted the ANU quad-rotor structure • Euler-Lagrange Formulation • PD Controller • Attitude and Altitude stabilization has been achieved [21] [22]
Quad-rotor Test bed	Ottawa University		• Newton-Euler Formulation • Fuzzy logic controller • Stabilized attitude and position [3]
DraganFlyer V Ti	Commercial		• Adopted this craft from Dragan Innovations Inc. • Euler-Lagrange equations used for mathematical modeling • PD controller has been implemented for the altitude and attitude [22]

3 Modeling and Simulation

This chapter addresses the general, common and particular characteristics and behaviors of a quad-rotor. It shows the relation between the governing forces, torques and others that affect their kinematics and dynamics.

'Modeling is the development of equations, constraints, and logic rules, while simulation is the exercising of the model'- ***Ingels***

Modeling and Simulation are fundamental tools in control engineering which are used in process of designing a new system, improving an already existing system or a model for which a controller has to be designed for.

Models are of different types to mention a few they could be verbal, action lists to be done, mathematical expressions or computer programs. Hence, from a control engineering point of view the type of model used is a mathematical model which is a representation of symbols, their meaning and manipulation of its exemplification by rules of logic and relating to a system's characterization [23]. These types of models are based essentially on the knowledge of the parameters important for that particular task.

There are also different types of simulations in relation to aircraft; the simulations could be for mission, surveillance, combat, dynamics, aerodynamics etc. from the point of the modeler.

In this thesis the Newton-Euler formulation is used to derive the equations of motions and has been verified in MATLAB-Simulink environment.

Figure 3-1 shows the steps followed in creating the model for a quad-rotor.

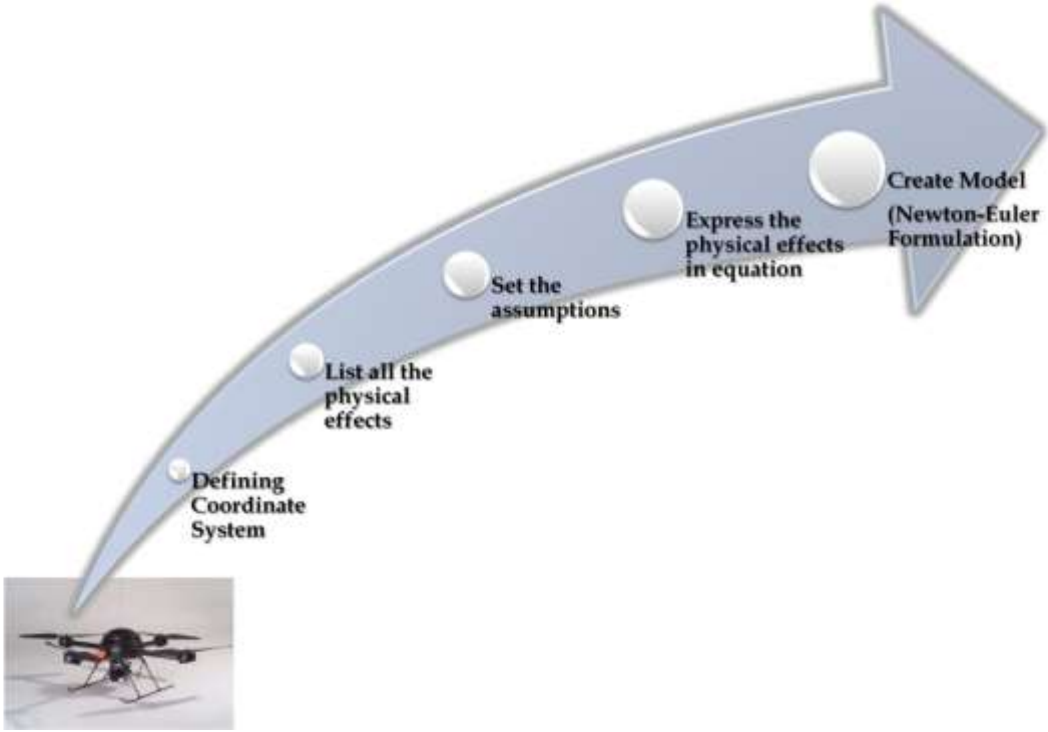

Figure 3-1: Steps followed in creating the model

3.1 Common Conventions

3.1.1 Frames of Reference

To define a position in a space a coordinate frame (system) should be defined [24]. A coordinate frame is defined by two things; one its origin should be specified in space and the other is its orientation should be specified. For this work, two frames of reference are used in order to define the position and orientation of the quad-rotor.

Unlike conventional rotorcrafts that use complex mechanisms to change blade pitch to direct thrust and steer the craft, the quad-rotor employs a much simpler differential thrust mechanism to control roll, pitch, and yaw. In order to track these attitude angles and changes to them while the craft is in motion, the use of two coordinate systems is required. [25]

One frame of reference is the inertial frame (IF) where it is considered to be stationary or moves with constant velocity. However, with respect to the second frame of reference which is the body fixed frame (BFF) i.e. the frame defined for the body at hand; it moves with a velocity of same magnitude but opposite in direction shown in Figure 3-2. The latter coordinate frame represents a rotating frame which follows the classical mechanics of Newton's law for angular motion.

The orientations of both frames is a North, East and Down convention which is a standard of aviation and both follow the right hand rule. Euler Angles (ϕ, θ, ψ) are used to describe the orientation of the rotating body fixed frame with respect to the inertial frame.

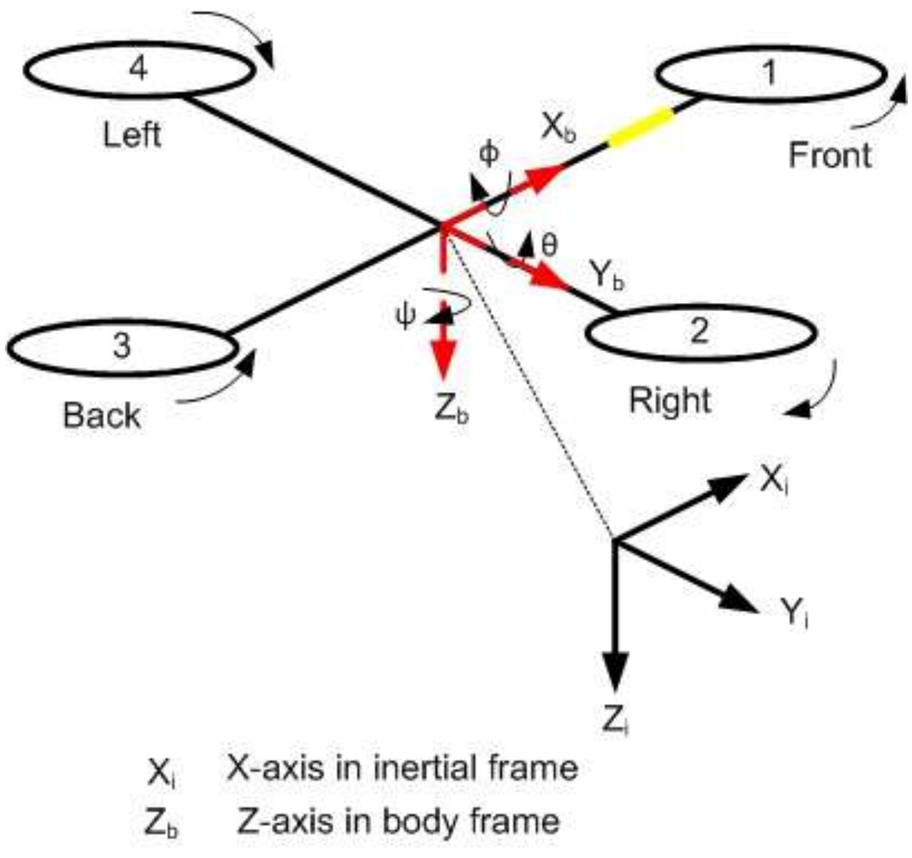

Figure 3-2: Inertial and Body Fixed Frame

The fore-arm that has a yellow mark indicates the front part of the body.

3.1.2 Rotation Matrix

A scheme of orienting a body to a desired orientation involves rotating three times successively about the axis of the body fixed frame. The sequence of rotating the body from BFF to IF results in a rotation matrix with a 1-2-3 sequence where the body is rotated from the Z-axis first and then the Y axis and finally the X-axis. The most powerful feature of the rotation matrix is its ability to directly project an arbitrary vector from one frame of reference to another.

$$R_B^I = \begin{bmatrix} C_\theta C_\psi & S_\phi S_\theta C_\psi - C_\phi S_\psi & C_\phi S_\theta C_\psi + S_\phi S_\psi \\ C_\theta S_\psi & S_\phi S_\theta S_\psi + C_\phi C_\psi & C_\phi S_\theta S_\psi - S_\phi C_\psi \\ -S_\theta & S_\phi C_\theta & C_\phi C_\theta \end{bmatrix} \qquad \textbf{3-1}$$

C_θ represents cosθ whereas S_θ represents sinθ. The Rotation matrix is used to relate the motions expressed in body-fixed frame with respect to the inertial frame.

Details of the successive rotations from the rotating frame to inertial frame are shown in Appendix A.

3.1.3 Transfer Matrix

This is the matrix used to relate the body angular rates to inertial angular rates; determined by taking the inverses of the individual rotations of the x and y axis.

$$T = \begin{bmatrix} 1 & S_\phi t_\theta & C_\phi t_\theta \\ 0 & C_\phi & -S_\phi \\ 0 & S_\phi Sec\theta & C_\phi Sec\theta \end{bmatrix} \qquad \textbf{3-2}$$

Details to the derivation of this matrix are shown in Appendix B.

3.1.4 Assumptions

The quad-rotor is quite easily modeled as a cross configuration with four rotors. The assumptions considered for modeling as listed as follows: [4], [10] etc.

- The propellers axes of rotation are fixed and parallel and the blades are fixed pitch. This assumption points out that the structure is rigid and the only things that vary are the propeller speeds.
- The cross configuration is symmetrical which points that the inertia tensor is a diagonal matrix and the inertia about the x-axis and the y-axis are equal.
- Centre of Gravity (CoG) and the body frame origin are assumed to coincide
- Interaction with ground or other surfaces is neglected
- Euler angles rates and body angular rates are considered equal near hover

3.2 Basic forces

Understanding the forces that affect the flight of aerial vehicles gives a clear picture about their dynamics. Generally, there are four basic forces that make the flight happen despite of the rotors that keep the vehicle up in the air. These forces push up, drag down, push forward and also slow the vehicle down and namely they are thrust, weight, lift and drag.

Thrust: is a force that moves the vehicle in the direction of motion; in our case for a rotorcraft it lifts it vertically and for a fixed wing it moves it forward overcoming the drag force which is considered as a frictional force. The increased speed of air flow on the upper surface produces decreased pressure and increases the pressure below the air foil. Combination of the differential pressure on both sides of the propeller generates an upward lift/thrust. [26]

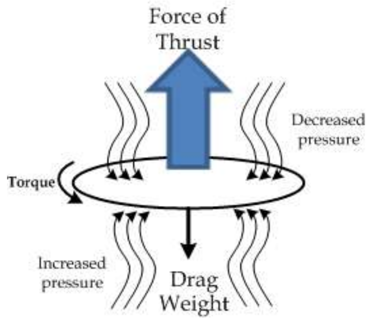

Figure 3-3: Ilustration about Thrust/Lift force

Weight: attraction by the gravitational force at the center of mass of the vehicle by the earth.

Lift: this force opposes the gravitational force; produced by the dynamic effect of air particles affecting the wings both on fixed-wing aircrafts and rotorcrafts.

Drag: is the force caused by difference in air pressure and friction i.e. it tends to slow an object. There are different kinds of drag forces namely, induced drag, form drag and Friction drag. The induced drag and Form drag are categorized under a pressure drag whereas the form drag and the friction drag are categorized under parasite drag. Form drag is a part of the parasite drag that is meant to say the drag that is not created due to friction. The pressure drag in general is due to a pressure against the surface.

3.3 *Physical Effects*

Physical effects are those forces or effects that arise because of the rotational nature of the craft. These effects mainly arise from the rotors, body movements in relation to the rotational reference frame whereas the other physical effect that has an impact on the motion is due to external environment.

Body Gyro effect: this effect is due to the centrifugal and coriolis forces that arise due to the cross coupling of the angular speeds.

Actuators action: this is the core effect that imposes on the dynamics and motion of the craft and action caused due to the variation of the propeller speeds which let the craft attain the desired orientation, height and position.

Disturbance: this has an impact in the dynamics of the craft by creating an imbalance in the motion and disorientation in the angles. It is generally caused usually through external environments.

3.4 Flight Conditions

- **Stationary (hover) flight**

Hovering is the flight condition where the rotorcraft UAV is in a stationary flight over a particular area (target); it generates its own gusty air but relatively to the surrounding wind it's low and very little aerodynamic forces act on it. It is usually called the challenging flight in flying a rotorcraft since it is against gravity, fuselage and flight control surfaces. This is the flight condition that will be addressed in this thesis. [27]

- **Translational flight**

This flight is between the hovering and cruising flight. This flight takes effect when the rotorcraft translates from a stationary flight to cruising flight where a translational lift takes place without power increase. [27]

- **Cruising (Forward) flight**

In contrast to the hovering flight here aerodynamic forces take effect; enable it to move forward. Forward motion is achieved in contrast to translational flight i.e. power is increased while maintaining airspeed whereas decreasing the power induces movement in the drag position. This flight condition is achieved the same for both rotorcraft and fixed-wing types. [27]

3.5 *Quad-rotor Dynamics*

In this section the key points that describe the behavior of UAVs and particularly quad-rotor is discussed.

Commonly UAVs including Quad-rotors are characterized by under actuated and coupled dynamics. Under actuated because they have six degrees of freedom (3 rotational and 3 translations) but have four actuated DoF and that the translational and rotational dynamics are coupled.

The equations of motion are governed by Newtonian mechanics and their evaluation is done through the appropriate choice of modeling technique i.e. Newton-Euler formulation.

3.5.1 Principle of Operation

A quad-rotor, as shown in the Figure 3-4, is a rotary wing UAV consisting of four rotors located at the ends of a cross (X) structure. Flight of quad-rotor is controlled by varying speed of each rotor. They have fixed-pitch blades and all their propellers axes of rotation are fixed and parallel. The assumptions that the structure is symmetrical and rigid point out that the only things that vary are the speeds of the propellers. Thus, the four basic movements (Lift/Thrust force, torque of Roll, torque of pitch and torque of yaw) are the targets that enable it to reach certain height and attitude. [10], [3]

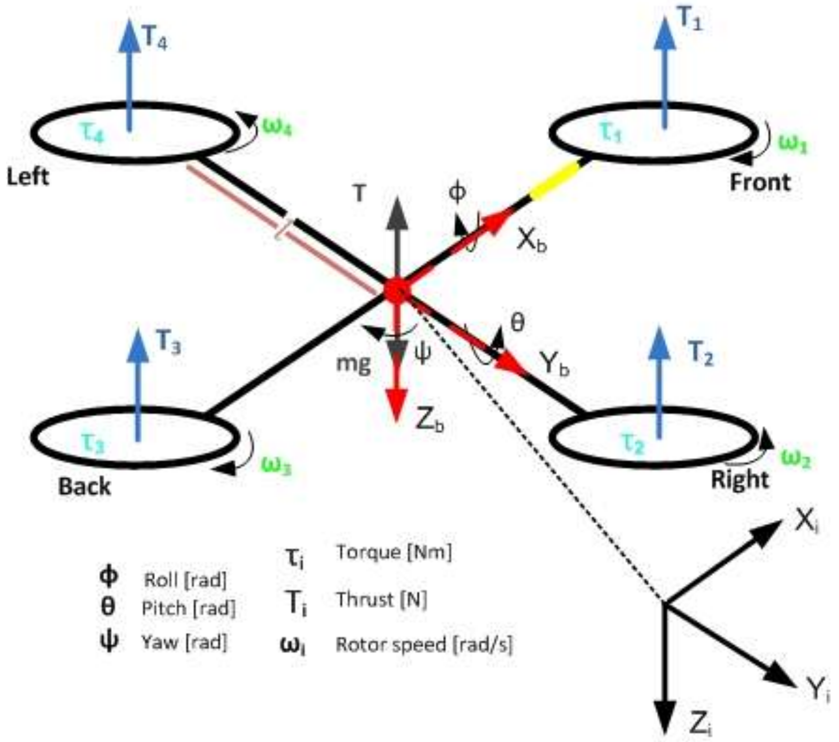

Figure 3-4: Conceptual Diagram of a Quad-rotor

As illustrated by the figure above, the top right rotor (Front) and bottom left rotor (Back) pair rotate in a clockwise direction, while the bottom right rotor (Right) and top left rotor (Left) pair rotate in a counter-clockwise direction. This configuration is devised in order to balance the drag created by each of the spinning rotor pairs; also enables balancing out of the reaction torques of the body due to the rotation of the propellers.

Behavior of a quad-rotor is depicted through the use of mathematical modeling, where this model is further used to develop a control law that results in achieving the desired motion. The kinematics and dynamics need to be first derived to fully formulate the mathematical model. [24]

The basic movements are described here: [10]

➢**Altitude**

This movement is portrayed by increasing (or decreasing) all propeller speeds (ω) simultaneously with the same rate. This leads to increasing or decreasing the thrust resulting in the raise or lowering of the quad-rotor vertically by overcoming the gravity respectively.

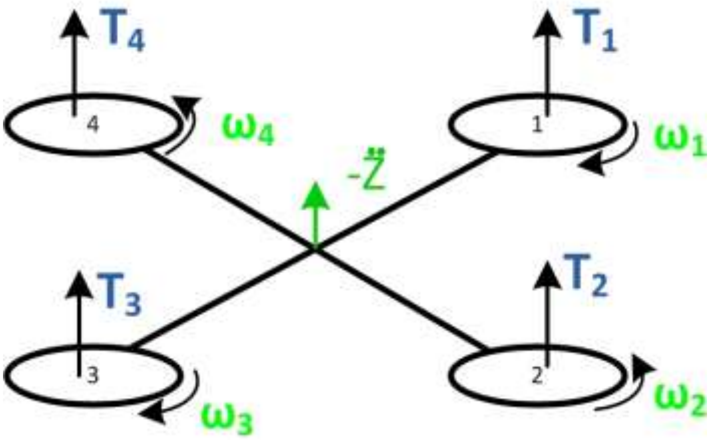

Figure 3-5: Thrust

The thrust generated is the total sum of all thrusts generated by the propellers; exactly canceling out the effect of gravity and velocity being zero at that instant. This is due to the equal propeller speed generation, ω_H[1], which allows the craft to maintain hovering position.

$$T_1 + T_2 + T_3 + T_4 = T_{total}$$

$$\omega_1 = \omega_2 = \omega_3 = \omega_4 = \omega_H$$

In Figure 3-5 and the forthcoming figures the basic movements are shown by illustrating the rotor speed through vector size. Size with a very bold arrow shows speed above average, the size which is small represents speed below average and average speed shown by a normal length of a line vector.

[1] Hovering speed

➢**Roll**

The movement roll is generated by increasing (or decreasing) the speed of the top left propeller (ω_4) and by decreasing (or increasing) the speed of the bottom right propeller (ω_2). A torque with respect to the BFF x-axis is generated where the quad-rotor turns with a roll (ϕ) angle. Keeping the thrust constant; roll motion can be achieved by manipulating the speeds of the bottom right and top left propellers. In the figure the arrow pointing to the left and right portrays the direction of the coupled translational motion.

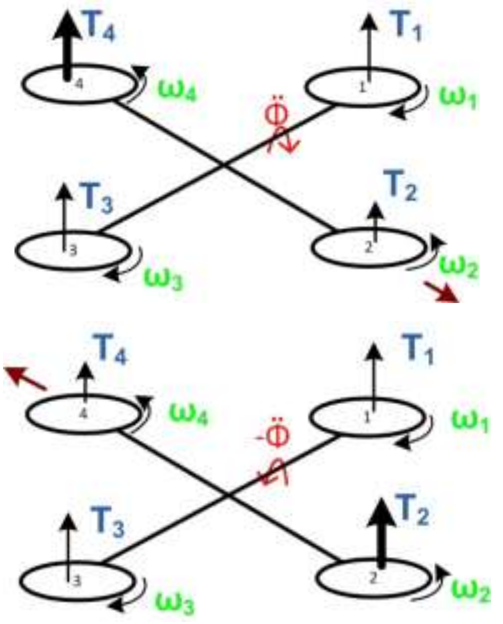

$$\omega_1 = \omega_3 - -\!\!\rightarrow T_1 = T_3$$

$$\omega_4 > \omega_2 - -\!\!\rightarrow T_4 > T_2$$

$$\omega_1 = \omega_3 - -\!\!\rightarrow T_1 = T_3$$

$$\omega_4 < \omega_2 - -\!\!\rightarrow T_4 < T_2$$

Figure 3-6: Roll

➢**Pitch**

The pitch movement is achieved by increasing (or decreasing) the bottom left propeller speed (ω_3) or by decreasing (or increasing) its pair propeller speed (ω_1). A torque with respect to the BFF y-axis is generated where the quad-rotor turns with a pitch angle (θ). While it's hovering pitch motion can be achieved by manipulating the speeds of the bottom left and top right propellers keeping the thrust constant. This movement is very similar to the roll motion with the manipulation of the other pair of propellers comes into action. In the figures below also here the arrow pointing from rotor 1 and 3 are the directions of the coupled translational motion.

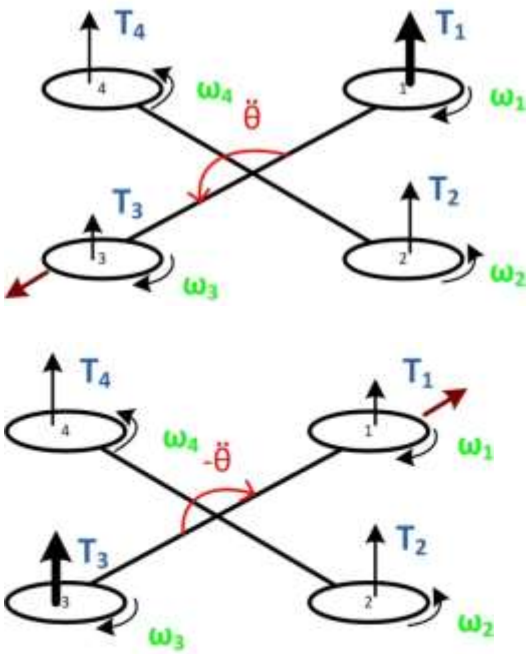

$$\omega_4 = \omega_2 - -\rightarrow T_4 = T_2$$

$$\omega_3 < \omega_1 - -\rightarrow T_3 < T_1$$

$$\omega_4 = \omega_2 - -\rightarrow T_4 = T_2$$

$$\omega_3 > \omega_1 - -\rightarrow T_3 > T_1$$

Figure 3-7: Pitch

➢**Yaw**

Increasing (or decreasing) the speed of the first pair i.e. top right and the bottom left (ω_1 & ω_3) and decreasing (or increasing) the speed of the other pair (ω_2 & ω_4) generates this movement. With this movement a torque with respect to the BFF z-axis is achieved where the quad-rotor turns clockwise (CW) or counter clockwise (CCW). The total thrust is the same as in hovering; but the total torque is unbalanced hence the quad-rotor turns itself around the z-axis of the body-fixed frame.

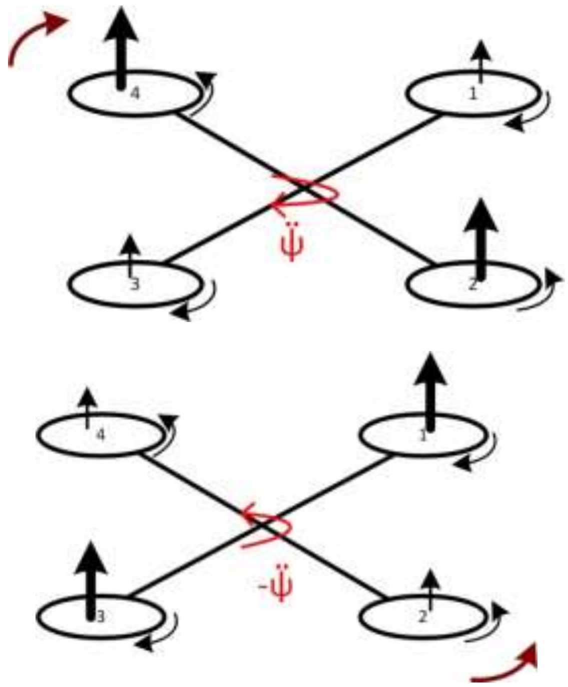

$$\omega_4 = \omega_2 --\rightarrow T_4 = T_2$$

$$\omega_3 = \omega_1 --\rightarrow T_3 = T_1$$

$$\omega_4 \& \omega_2 > \omega_3 \& \omega_1$$

$$\omega_4 = \omega_2 --\rightarrow T_4 = T_2$$

$$\omega_3 = \omega_1 --\rightarrow T_3 = T_1$$

$$\omega_4 \& \omega_2 < \omega_3 \& \omega_1$$

Figure 3-8: Yaw

It should be noted that whenever a thrust differential causes the quad-rotor to pitch or roll, the total thrust vector decreases because it is inclined away from the vertical i.e. the thrust vector is then resolved into horizontal and vertical component, which leads the quad-rotor to descend. [28]

Ascend and Descend

By increasing or decreasing the thrust from each rotor by the same amount altitude is controlled but the total torque on the body remains zero.

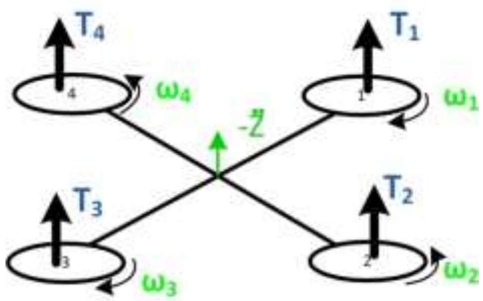

$$(\omega_1 = \omega_2 = \omega_3 = \omega_4) > \ \omega_H$$

Above average speed enables ascending

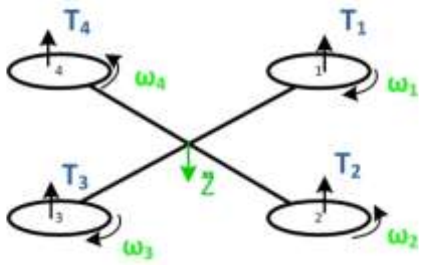

$(\omega_1 = \omega_2 = \omega_3 = \omega_4) < \omega_H$

Below average speed enables descending

Figure 3-9: Ascend (top), Descend (bottom)

In section 3.6 the basic four movements mentioned above shall be verified together with the depicted model of the dynamic system.

3.5.2 Equations of motion

Equations of motion of physical dynamic systems such as Unmanned Aerial Vehicles (UAVs) are described by the Newton-Euler formalism; the common and important terminology used in describing these motions is the definition of the frame of reference discussed in the previous section.

Two frames of reference are used for the dynamics; one that is fixed (inertial frame) and the other fixed to the body of the quad-rotor (body-fixed frame). Rotation matrix is used to correctly apply Newton's laws of motion since almost all measures are with respect to the body-fixed frame except gravity, thus, this matrix is used to relate the motions expressed in body-fixed frame with respect to the inertial frame.

North-East-Down convention was chosen for the frames of reference as it complies with standard aviation system and satisfies the right hand rule.

The Euler angles (ϕ, θ, ψ), angular velocities, linear position and linear velocities makeup the attitude w.r.t the BFF and relationship of the quad-rotor w.r.t the IF respectively making up twelve state variables.

$$X = \begin{bmatrix} x & \dot{x} & y & \dot{y} & z & \dot{z} & \phi & \dot{\phi} & \theta & \dot{\theta} & \psi & \dot{\psi} \end{bmatrix}' \qquad \textit{3-3}$$

In Equation 3-3; $(\phi, \dot{\phi}, \theta, \dot{\theta}, \psi, \dot{\psi})$ are the 6 state variables that make up the attitude of the craft with respect to the body fixed frame and the rest 6 state variables i.e. $(x, \dot{x}, y, \dot{y}, z, \dot{z})$ define the relationship of the craft with the inertial frame; these include the physical location of the craft within the inertial coordinate system along each of its principal axes including the velocities in these directions.

Understanding and accounting for the various forces and moments induced on the quad-rotor is important in order to create an accurate model. With the general Newton's law of motion, individual forces and moments are defined for each degree of freedom and full equations of motion of the quad-rotor can be determined by using the Newton-Euler formalism.$F = ma$; $\tau = I\alpha$

$$\begin{bmatrix} F_x \\ F_y \\ F_z \end{bmatrix} = \begin{bmatrix} m & 0 & 0 \\ 0 & m & 0 \\ 0 & 0 & m \end{bmatrix} \begin{bmatrix} a_x \\ a_y \\ a_z \end{bmatrix}$$

3-4

$$\begin{bmatrix} \tau_x \\ \tau_y \\ \tau_z \end{bmatrix} = \begin{bmatrix} I_{xx} & 0 & 0 \\ 0 & I_{yy} & 0 \\ 0 & 0 & I_{zz} \end{bmatrix} \begin{bmatrix} \alpha_x \\ \alpha_y \\ \alpha_z \end{bmatrix}$$

For a rotating frame of reference it is common that centrifugal and coriolis forces arise due to rotation according to the laws of motion by Newton; these forces do not arise if the frame of reference is at rest. [29]

Generally, the equation below relates the rates of change of any vector in a fixed and rotating frame; also as seen from [24], [29] applies to any vector quantity and is fundamental importance to dynamic problems where a rotating reference frame is involved.

$$\left\{\frac{d\vec{r}}{dt}\right\}_A = \left\{\frac{d\vec{r}}{dt}\right\}_U + \vec{\omega}_{UA}\ X\ \vec{r} \qquad \textbf{3-5}$$

The concept behind the equation written above is that; as the unit vector r fixed in the reference (body fixed) frame U rotates with an angular velocity $\vec{\omega}_{UA}$ with respect to A (inertial) reference frame. The rate of change of the unit vector r is caused only by $\vec{\omega}_{UA}$ and it must be normal to both the unit vector and angular velocity

Here the rotation and translation matrices in a BFF are combined and based on Equation (3-6) the coriolis terms/forces are picked up when the linear velocities are crossed (vector product) with the angular velocities.

The Newton –Euler Equation [10] that is used to derive the equations of motion is written below.

$$m\vec{v} + wx\vec{v} = F$$

$$\begin{bmatrix} mI_{3x3}{}^{2} & 0_{3x3} \\ 0_{3x3} & I_{xyz} \end{bmatrix} \begin{bmatrix} \dot{v}^B \\ \dot{w}^B \end{bmatrix} + \begin{bmatrix} w^{B^3}\ x\ (mv^B) \\ w^B\ x\ \left(I_{xyz}w^B\right) \end{bmatrix} = \begin{bmatrix} F^B \\ \tau^B \end{bmatrix} \qquad \textbf{\textit{3-6}}\ \text{(a,b)}$$

Since weight is force and not torque it only affects the translational motion and below it is expressed w.r.t the BFF.

$$Weight_{BFF} = R^{-1}Weight_{IF}$$

$$R^{-1} = R'^{\,4} \qquad \textbf{\textit{3-7}}$$

$$Weight_{BFF} = \begin{bmatrix} -mgsin\theta \\ mgcos\theta sin\phi \\ mgcos\theta cos\phi \end{bmatrix}$$

The Euler rates w.r.t the IF and the body-axis rates w.r.t the BFF are related using the transfer matrix.

---

[2] I_{3x3} indicates an identity matrix which has a 3 by 3 dimension
[3] Superscript B indicates the variables w.r.t the BFF.
[4] The inverse of the rotation matrix is equal to its transpose because the matrix is orthonormal.

$$\begin{bmatrix} \dot{\phi}_b \\ \dot{\theta}_b \\ \dot{\psi}_b \end{bmatrix} = T^{-1} \begin{bmatrix} \dot{\phi} \\ \dot{\theta} \\ \dot{\psi} \end{bmatrix}^{5} \qquad \textbf{3-8}$$

The generic form of Force and Torque of a 6 DoF rigid body [4] is described here:

$$F^B_{total} = -F^B_{thrust} + F^B_{weight} + F^B_{aerodynamics} + F^B_{disturbance}$$

$$\tau^B_{total} = Gyroscopic_{effects} + Actuators + \tau^B_{aerodynamics} + \tau^B_{disturbance} \qquad \textbf{3-9}$$

For now the aerodynamic forces and the disturbance forces are neglected; and the acceleration of the quad-rotor (both the linear and angular accelerations) is determined by substituting equations (coriolis and the movement vectors) into the generic equation.

Generally the governing equations of motion as defined in the body fixed frame are written here below:

$$\begin{bmatrix} \ddot{x}_b \\ \ddot{y}_b \\ \ddot{z}_b \end{bmatrix} = \begin{bmatrix} 0 \\ 0 \\ \frac{-F_{thrust}}{m} \end{bmatrix} + g \begin{bmatrix} -sin\theta \\ cos\theta sin\phi \\ cos\theta cos\phi \end{bmatrix} - \begin{bmatrix} \dot{\theta}\dot{z} - \dot{\psi}\dot{y} \\ \dot{\psi}\dot{x} - \dot{x}\dot{z} \\ \dot{\phi}\dot{y} - \dot{\theta}\dot{x} \end{bmatrix}$$

$$\begin{bmatrix} \ddot{\phi}_b \\ \ddot{\theta}_b \\ \ddot{\psi}_b \end{bmatrix} = \left[- \begin{bmatrix} (I_{zz} - I_{yy})\dot{\theta}\dot{\psi} \\ (I_{xx} - I_{zz})\dot{\psi}\dot{\phi} \\ (I_{yy} - I_{xx})\dot{\phi}\dot{\theta} \end{bmatrix} + \begin{bmatrix} \tau_\phi \\ \tau_\theta \\ \tau_\psi \end{bmatrix} \right] \begin{bmatrix} 1/I_{xx} \\ 1/I_{yy} \\ 1/I_{zz} \end{bmatrix} \qquad \textbf{3-10}$$

In Equation 3-10, we see the equations of motion described in the body fixed frame.

The maneuvers executed by the quad-rotor are resultants from the manipulation of the thrust and drag moment created by the four rotors. The thrust (b) and drag (d) coefficients are derived from the blade element theory from the work of [19] and (*l*) is the length of the

5

$$T = \begin{bmatrix} 1 & S_\phi t_\theta & C_\phi t_\theta \\ 0 & C_\phi & -S_\phi \\ 0 & S_\phi Sec\theta & C_\phi Sec\theta \end{bmatrix}; T^{-1} = \begin{bmatrix} 1 & 0 & S_\theta \\ 0 & C_\phi & S_\phi C_\theta \\ 0 & -S_\phi & C_\phi C_\theta \end{bmatrix}$$

arm between the CoG and the tip where rotor is placed. The parameters have the relationship shown in equation 3-11 .

$$F = b\omega_i^2$$

$$\tau = d\omega_i^2 \qquad \textbf{\textit{3-11}}$$

Equation (3-11) shows that by controlling the rotational speed of the motors one can effectively control the rotorcraft; hence, the following actions of movements were chosen as the control inputs. [21]

$$F_{thrust}(\omega_i) = b(\omega_1^2 + \omega_2^2 + \omega_3^2 + \omega_4^2) = u_1; i = 1 - 4$$

$$\tau_\phi(\omega_{2,4}) = bl(\omega_4^2 - \omega_2^2) = u_2 \qquad \textbf{\textit{3-12}}$$

$$\tau_\theta(\omega_{1,3}) = bl(\omega_1^2 - \omega_3^2) = u_3 \qquad \text{(a,b,c,d)}$$

$$\tau_\psi(\omega_i) = d(-\omega_1^2 + \omega_2^2 - \omega_3^2 + \omega_4^2) = u_4; i = 1 - 4$$

It is quite easier to express the dynamics in inertial frame for control in particular for the position and the rotational has no significance difference when expressed in inertial frame since the transfer matrix that relates the angular body rates to the angular rates in the inertial frame is equivalent to an identity matrix since the craft is in hovering position; hence, remains the same. Therefore; the model (governing equations) expressed in inertial frame is outlined in the equation below:

$$\dot{x} = f(x, u) \qquad \textbf{\textit{3-13}}$$

$$\begin{bmatrix} \dot{x}_I \\ \ddot{x}_I \\ \dot{y}_I \\ \ddot{y}_I \\ \dot{z}_I \\ \ddot{z}_I \end{bmatrix} = \begin{bmatrix} x_2 \\ (-(cos\phi sin\theta cos\psi + sin\phi sin\psi)\ F\_thrust)/m \\ x_4 \\ (-(cos\ \phi sin\theta sin\psi\ - sin\phi cos\psi\ )F\_thrust)/m) \\ x_6 \\ g - (((cos\phi cos\theta)F\_thrust)/m) \end{bmatrix} \qquad \textbf{\textit{3-14}}$$

$$\begin{bmatrix} \dot{\phi}_I \\ \ddot{\phi}_I \\ \dot{\theta}_I \\ \ddot{\theta}_I \\ \dot{\psi}_I \\ \ddot{\psi}_I \end{bmatrix} = \begin{bmatrix} x_8 \\ \frac{(I_{yy}-I_{zz})}{I_{xx}}\dot{\theta}\dot{\psi} + \frac{\tau_\phi}{I_{xx}} \\ x_{10} \\ \frac{(I_{zz}-I_{xx})}{I_{yy}}\dot{\phi}\dot{\psi} + \frac{\tau_\theta}{I_{yy}} \\ x_{12} \\ \frac{(I_{xx}-I_{yy})}{I_{zz}}\dot{\phi}\dot{\theta} + \frac{\tau_\psi}{I_{zz}} \end{bmatrix} \tag{3-15}$$

Equations 3-14 and 3-15 show the equations of motion with respect to the inertial frame.

Reducing the model to a suitable format for the controller is linearizing the equations of motion at an operating point where the craft is hovering. While the craft is in hovering position the angles particularly the roll and pitch angles should be stabilized i.e. both angles should be zero so that there would be no movement in the x and y translational motion since they are coupled; whereas the lateral (x-), longitudinal (y-), altitude (z-) and the orientation (yaw angle ψ-) could be a constant. For this work, the equilibrium point taken and the assumed operating point; written below in equation (3-16) and at this operating point the governing equations of motion are deduced.

$$x_{eq} = [x, 0, y, 0, z, 0,0,0,0,0, \psi, 0]'$$

$$= [0,0,0,0,-8,0,0,0,0,0,0,0]'$$

3-16 (a , b)

$$u_{eq} = [u_1, u_2, u_3, u_4]'$$

where at hovering $u_{1eq} = mg = F_{thrust}$

x_{eq} and u_{eq} are the equilibrium points where the craft is linearized at hovering position.

Using the above operating point; the state space form of the equations of motion is

$$\dot{x} = Ax + Bu$$

$$y = Cx \tag{3-17}$$

Where; $A = \frac{\partial f}{\partial x}|_{x=x_{eq}}$; $B = \frac{\partial f}{\partial u}|_{u=u_{eq}}$

$$A = \begin{bmatrix} 0 & 1 & 0 & 0 & 0 & 0 & 0 & 0 & 0 & 0 & 0 & 0 \\ 0 & 0 & 0 & 0 & 0 & 0 & 0 & 0 & -g & 0 & 0 & 0 \\ 0 & 0 & 0 & 1 & 0 & 0 & 0 & 0 & 0 & 0 & 0 & 0 \\ 0 & 0 & 0 & 0 & 0 & 0 & g & 0 & 0 & 0 & 0 & 0 \\ 0 & 0 & 0 & 0 & 0 & 1 & 0 & 0 & 0 & 0 & 0 & 0 \\ 0 & 0 & 0 & 0 & 0 & 0 & 0 & 0 & 0 & 0 & 0 & 0 \\ 0 & 0 & 0 & 0 & 0 & 0 & 0 & 1 & 0 & 0 & 0 & 0 \\ 0 & 0 & 0 & 0 & 0 & 0 & 0 & 0 & 0 & 0 & 0 & 0 \\ 0 & 0 & 0 & 0 & 0 & 0 & 0 & 0 & 0 & 1 & 0 & 0 \\ 0 & 0 & 0 & 0 & 0 & 0 & 0 & 0 & 0 & 0 & 0 & 0 \\ 0 & 0 & 0 & 0 & 0 & 0 & 0 & 0 & 0 & 0 & 0 & 1 \\ 0 & 0 & 0 & 0 & 0 & 0 & 0 & 0 & 0 & 0 & 0 & 0 \end{bmatrix}$$

$$B = \begin{bmatrix} 0 & 0 & 0 & 0 \\ 0 & 0 & 0 & 0 \\ 0 & 0 & 0 & 0 \\ 0 & 0 & 0 & 0 \\ 0 & 0 & 0 & 0 \\ -\frac{1}{m} & 0 & 0 & 0 \\ 0 & 0 & 0 & 0 \\ 0 & \frac{l}{i_{xx}} & 0 & 0 \\ 0 & 0 & 0 & 0 \\ 0 & 0 & \frac{l}{i_{yy}} & 0 \\ 0 & 0 & 0 & 0 \\ 0 & 0 & 0 & \frac{1}{i_{zz}} \end{bmatrix} \qquad \textbf{\textit{3-18}} \; (a,b,c)$$

$$C = \begin{bmatrix} 1 & 0 & 0 & 0 & 0 & 0 & 0 & 0 & 0 & 0 & 0 & 0 \\ 0 & 0 & 1 & 0 & 0 & 0 & 0 & 0 & 0 & 0 & 0 & 0 \\ 0 & 0 & 0 & 0 & 1 & 0 & 0 & 0 & 0 & 0 & 0 & 0 \\ 0 & 0 & 0 & 0 & 0 & 0 & 1 & 0 & 0 & 0 & 0 & 0 \\ 0 & 0 & 0 & 0 & 0 & 0 & 0 & 0 & 1 & 0 & 0 & 0 \\ 0 & 0 & 0 & 0 & 0 & 0 & 0 & 0 & 0 & 0 & 1 & 0 \end{bmatrix}$$

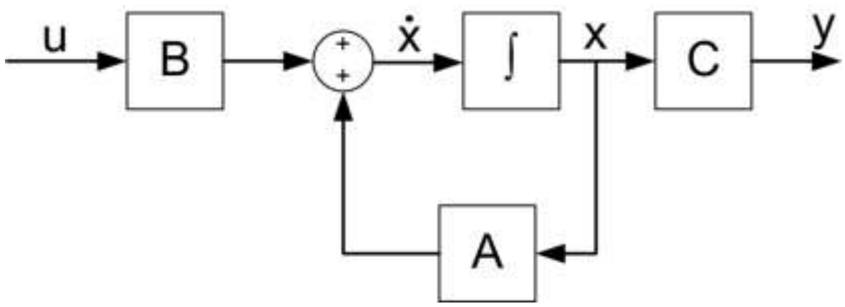

Figure 3-10: Generic State space model

3.6 Model Verification

In the previous section it has been understood what the principle of operation of a quad-rotor UAV are and the equations of motion has been based on the Newton-Euler formulation. Here it has been tried to show whether the model adheres to the concepts pointed out in the operation and faithfully respond to the inputs it is commanded with. As it can be seen from Figure 3-11; the model is shown using a Simulink block modeling scheme.

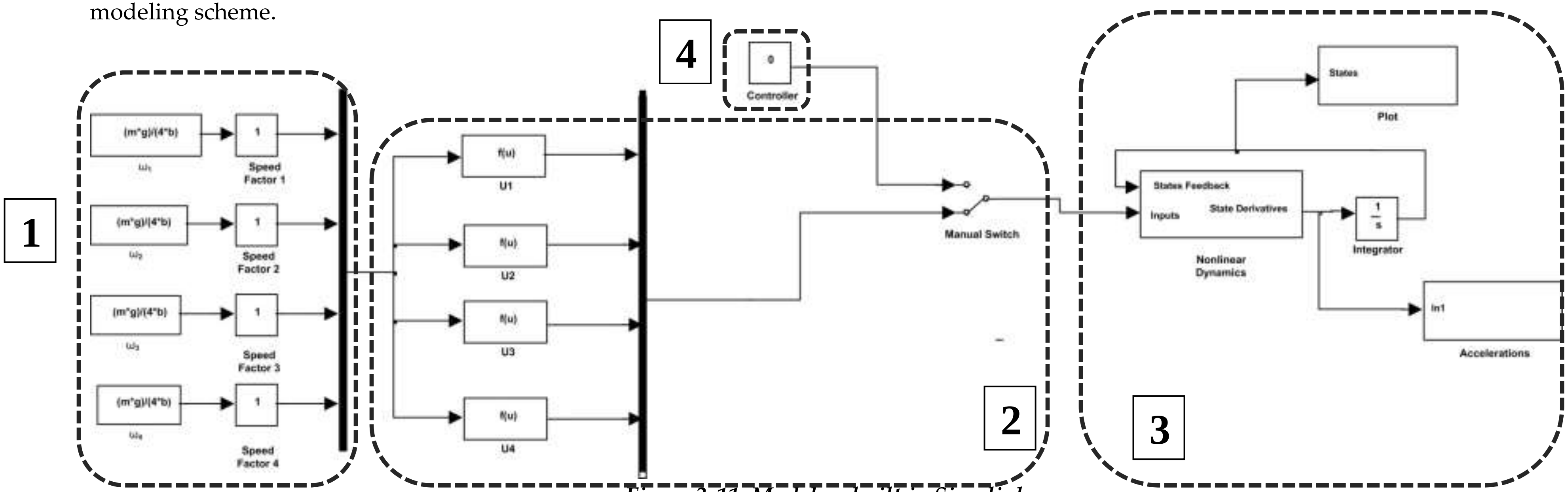

Figure 3-11: Model as built in Simulink

From left to right here the model is divided into four parts; these are described as follows:

Block 1: shows that there are about four constant blocks which have held the speed of the propeller which is an essential input to the dynamics from which the Thrust, torque of roll, torque of Pitch and torque of yaw are calculated to give the 6DoF of the quad rotor. It is also known that for a hover flight regime the speed of the propeller on each rotor should be about the average hence to represent this condition a slider gain representing speed factor with 0 being its minimum (Low Speed) and 2 its maximum (Full Speed) has been included to the model; hence 1 (Average Speed) being the average multiplier of the propeller's speed that lets the quad rotor be in the stationary flight (Hovering) condition.

Block 2: The second block from the model has two components; the command inputs and the manual switch. The manual switch is used as an Open/Closed loop switch which we tend to use when a controller is incorporated in to the model to control the position and attitude of the system at hovering position (scope for this thesis) by manipulating the control inputs. And the command inputs are those that drive the motion of the craft by reaching to a required propeller speed.

Block3: the core of the system is shown in this block. Here the dynamics of the quad rotor has been incorporated using the MATLAB function block and the output of this block are the state derivatives which are shown with a scope in the accelerations block for both the linear and angular acceleration; whereas the integrator is used to output the state vector which is used in the dynamics and a vital input to plots block (where the 6 DoF are plotted for different inputs) in turn it is also fed back to the dynamics block as a state feedback.

Block 4: this block from the model has the controller part where it is represented by a constant i.e. zero to indicate that there is no controller but just the model of the system to be premeditated which will come into the picture after the controller is designed.

The parameters used for this work are adopted from [1] and have been attached on Appendix C.

The work done here is for the quad rotor at hovering position; as learnt from the dynamics of the rotorcraft at hovering position each propeller has the same speed i.e. each propeller is at the average speed simultaneously. At this point since the force and torque reacting to the rotorcraft are balanced; on equation (3-19) it is shown that the total uplift thrust developed by the four rotors balances the rotorcraft weight and the counter torque developed are canceled out.

$$T = mg \qquad \textbf{3-19}$$

Where, $T = b(\omega_1^2 + \omega_2^2 + \omega_3^2 + \omega_4^2)$

But we have said that at hovering position the propeller speeds are all equal ($|\omega_1| = |\omega_2| = |\omega_3| = |\omega_4|$)

Therefore; $\omega = \sqrt{\frac{mg}{4b}}$ with this propeller speed at each rotor the quad rotor has the condition of stationary flight.

Where; mg is the weight/force of gravity acting on the quad rotor from the inertial frame.

Below figures for an open loop model of the system for different inputs are shown.

- **Scenario One: Descending Speed**

When the propellers are at Low speed ($\omega_i = s_f * \omega_H$); for i=1-4; i is the number of rotors. ω_H represents the average speed which corresponds to hovering speed at which the quad rotor is at stationary flight whereas S_f represents the speed factor below hovering speed ($s_f < 1$) for which the craft starts descending. Matrix showing the respective hovering position assumed is written below.

$$\begin{bmatrix} x \\ y \\ z \\ \phi \\ \theta \\ \psi \end{bmatrix} = \begin{bmatrix} 0 \\ 0 \\ -8 \\ 0 \\ 0 \\ 0 \end{bmatrix}$$

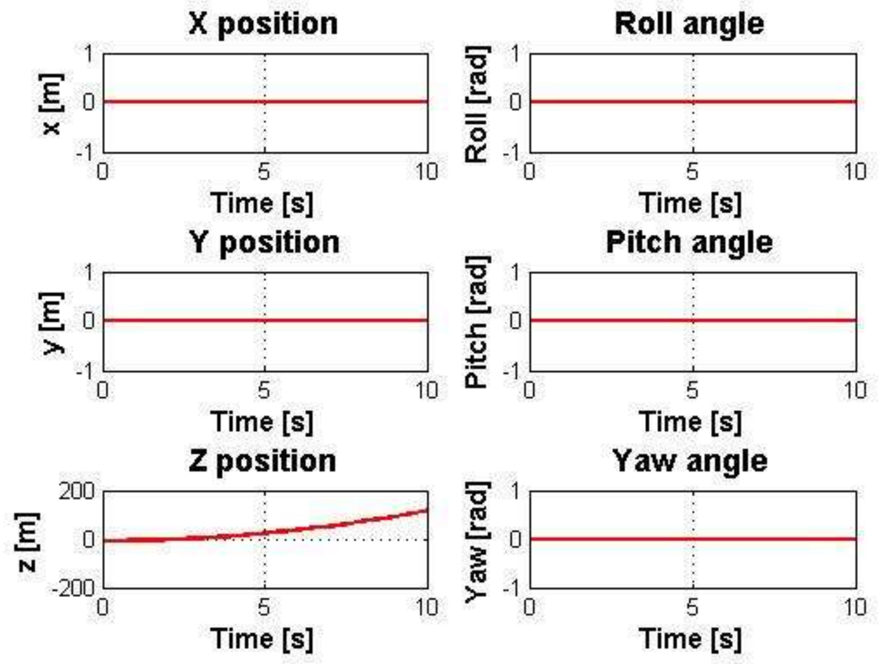

Figure 3-12: Quad-rotor descending

This figure shows that all except the altitude are zero implicating that the rotors are rotating at low speed. The altitude (Z position figure) illustrates that from hovering position when the propeller speeds are below the average (hovering) speed the rotorcraft starts falling below the intended hovering position.

- **Scenario Two: Ascending Speed**

When the propellers are at ascending speed ($\omega_i = s_f * \omega_H$); for i=1-4. ω_H represents the average speed which corresponds to hovering speed at which the quad rotor is at stationary flight whereas S_f represents the speed factor above hovering speed ($s_f > 1$) for which the craft starts ascending.

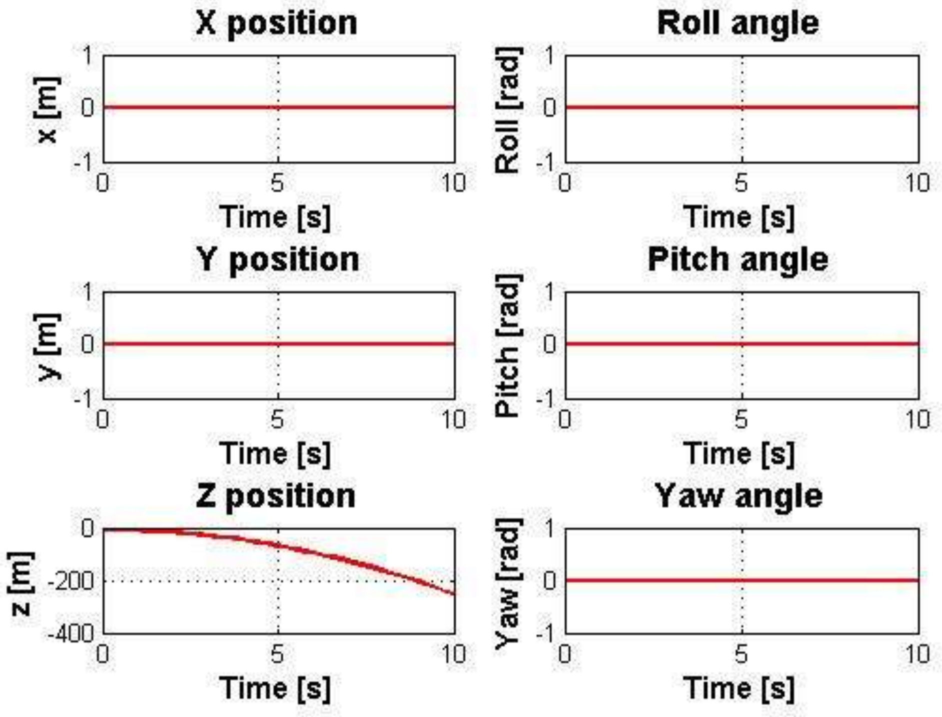

Figure 3-13: Quad-rotor Ascending

This plot shows that at ascending speed the lifting force or thrust takes over the weight leading the quad rotor to ascend from the point where it hovers with the average speed which is shown in the next scenario. Other than the altitude (Z position) all other degrees of freedom have no change as long as all propeller speeds are increasing or decreasing at the same speed simultaneously.

- **Scenario Three: Average/Hovering Speed**

When the propellers are at average speed ($\omega_i = s_f * \omega_H$); for i=1-4. ω_H represents the average speed which corresponds to hovering speed at which the quad rotor is at stationary flight whereas S_f represents the speed factor equal to hovering speed ($s_f = 1$) for this scenario where the craft hovers.

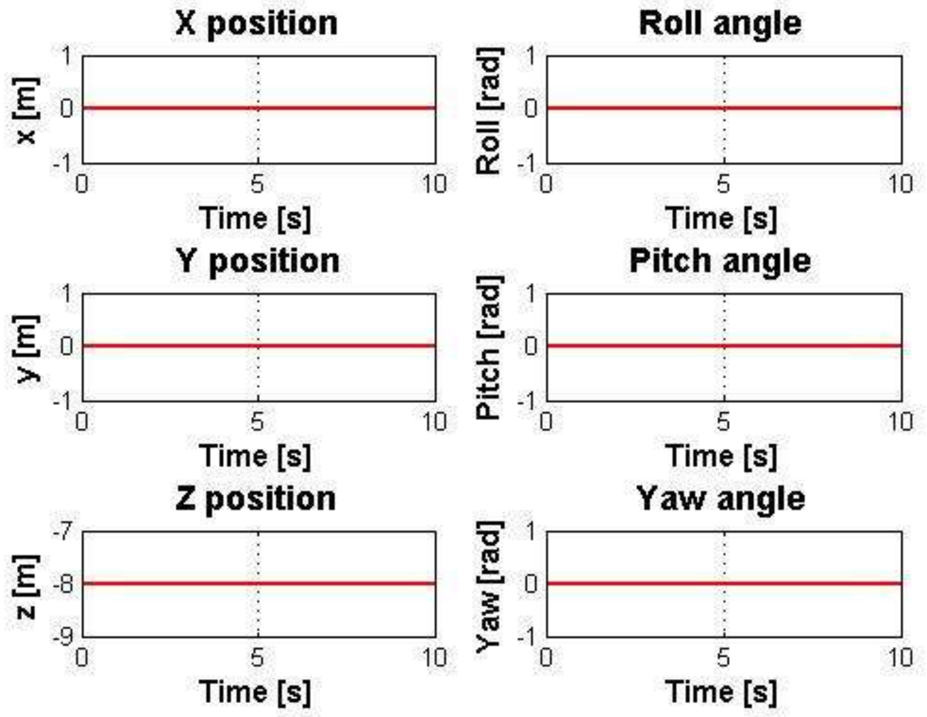

Figure 3-14: Quad-rotor Hovering at zero equilibrium point

The above plot shows that at average speed, the thrust and weight are equal which implies that for this flight condition the force and torque are balanced. All 6 DoF are at the assumed hovering position i.e. the operating point; with this propeller speed the hovering flight condition is achieved where all positions and angles are maintained.

- **Scenario Four: Roll**

This dynamics is obtained by decreasing (or increasing) the left-right propeller speed while maintaining hovering speed for the front-back propeller. With this dynamics we can understand that the roll angle and the Y position are coupled. Below the two figures show the roll movement of the quad rotor by performing either of the above variations on the propeller speed.

($\omega_4 = s_f * \omega_H$); s_f<1 and ($\omega_2 = s_f * \omega_H$); s_f>1 implies rolls to the left while ($\omega_i = s_f * \omega_H$); i=1 and 3 and the s_f =1 implying this pair of rotors are still at hovering speed.

For the quad rotor to roll to the right the opposite operation i.e. the left (4th rotor) shall have speed above the hovering speed factor and that of the right (2nd rotor) shall be decreased from the average/hovering speed. And the craft is initially hovering at 8m.

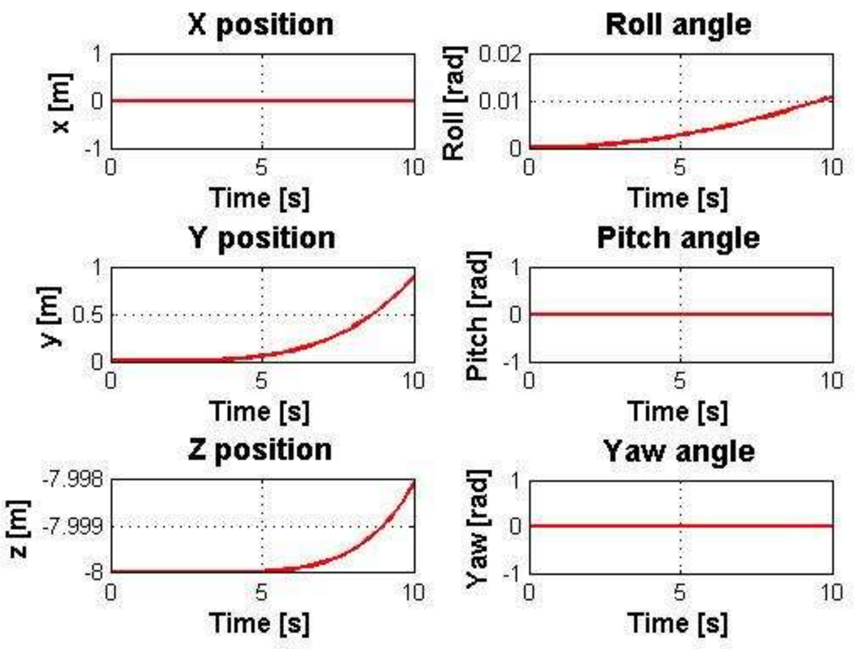

Figure 3-15: Quad-rotor Rolling to the right

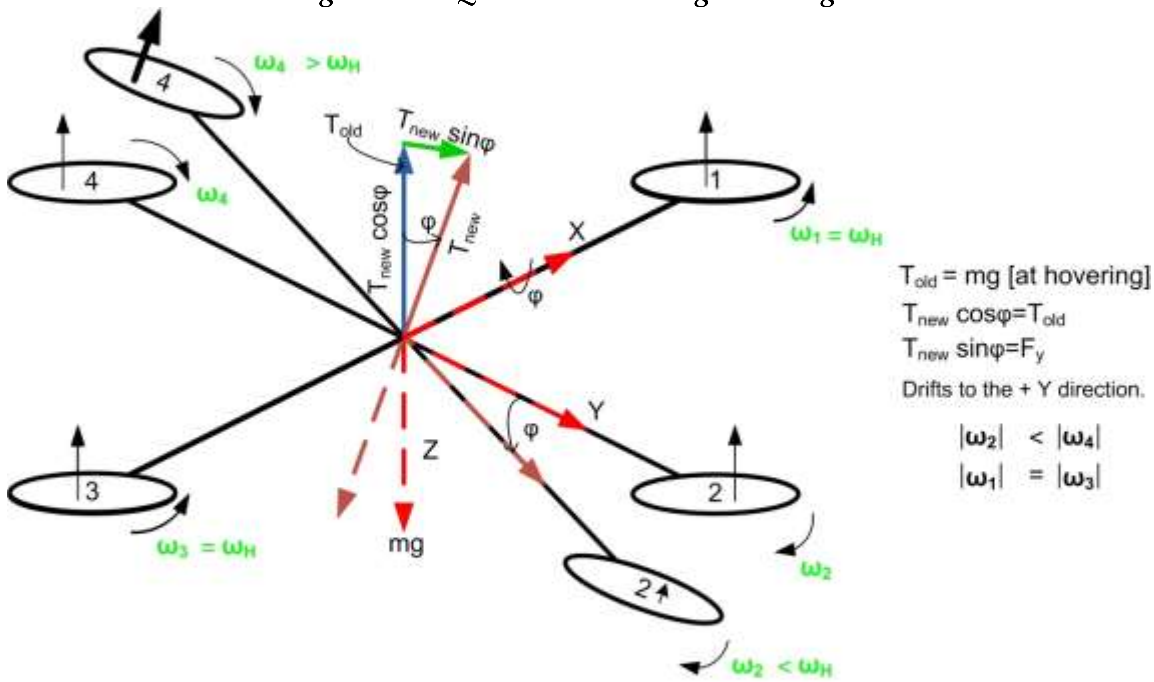

Figure 3-16: Force decomposition showing ϕ and Y drfit are coupled

On the figures from the previous page the following is seen:

When the propeller speed of the right rotor is decreased and conversely the speed of the left rotor is increased; the rotorcrafts rolls to the right. While rolling the height is a slightly over thrown from the hovering position in order to balance the rolling effect. In this scenario we also see that the Y position coupled to the rolling angle is positive and has a drift to its positive; in its direction of orientation similar to its respective angle.

- **Scenario five: Pitch**

This dynamics is obtained by decreasing (or increasing) the front-back propeller speed while maintaining hovering speed for the front-back propeller. With this dynamics we can understand that the pitch angle and the X position are coupled. Below the two figures show the pitching movement of the quad rotor by performing either of the above variations on the propeller speed.

$(\omega_3 = s_f * \omega_H)$; s_f<1 and $(\omega_1 = s_f * \omega_H)$; sf >1 implies the craft pitches backward while $(\omega_i = s_f * \omega_H)$; i=2 and 4 and the s_f =1 inferring this pair of rotors are still at hovering speed.

For the quad rotor to pitch forward the opposite operation i.e. the back (3rd rotor) shall have speed above the hovering speed factor and that of the front (1st rotor) shall be decreased from the average/hovering speed. The quad-rotor was initially hovering at 8m until it starts pitching due to the variation is speed with respect to the rotors that make the change.

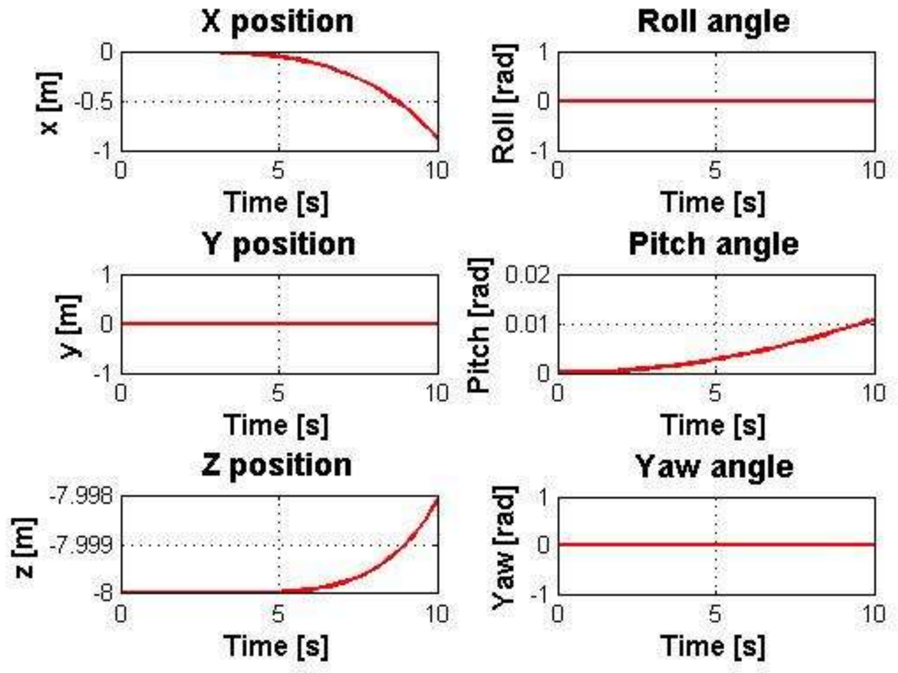

Figure 3-17: Quad-rotorpitching to forward

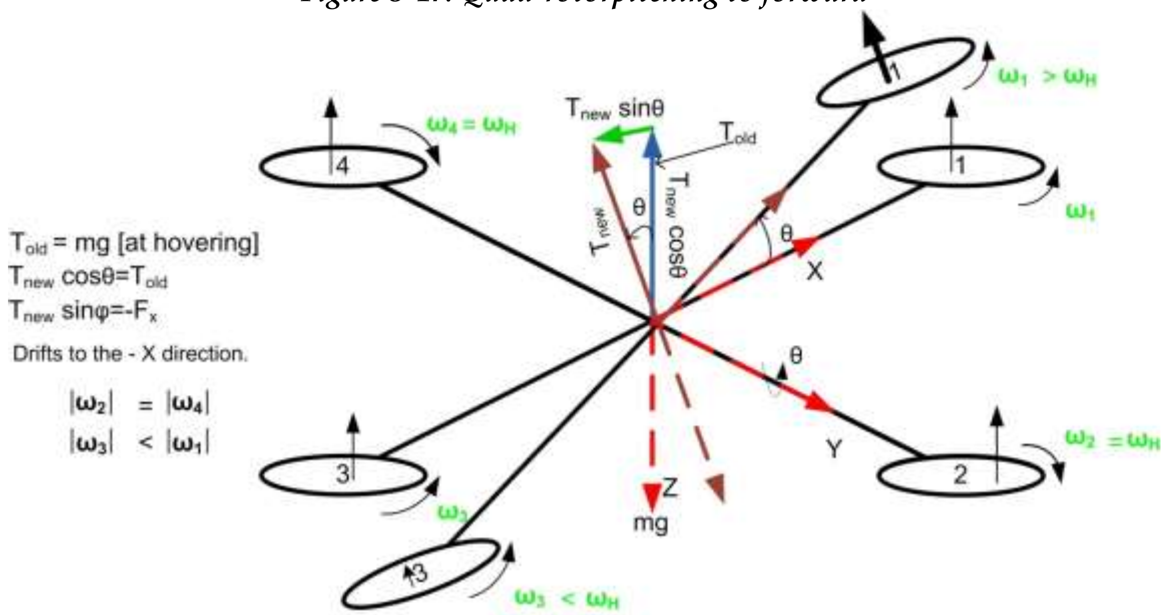

Figure 3-18: Force decomposition showing that θ and X drift are coupled

On the previous page from the figures we see the following concept:

When the propeller speed of the front rotor is decreased and the back is increased the rotorcraft pitches forward maintaining the vertical thrust in hover position with a change in the height because the balance would be a bit over thrown while pitching. In this scenario we also see that the X position coupled to the Pitch angle is negative and has a drift to its positive; in its direction of orientation.

- **Scenario Six: Yaw**

This dynamics is obtained by decreasing (or increasing) the left-right propellers speed while increasing (or decreasing) the front-back propeller speed keeping the overall thrust the same. Below the figure shows the yaw movement of the quad rotor by performing either of the above variations on the propeller speed.

($\omega_i = s_f * \omega_H$); sf <1 for i=1 and 3 and ($\omega_j = s_f * \omega_H$); sf >1 for j=2 and 4 implies the craft yaws to the clockwise while maintaining the total thrust as it was in hovering position i.e. balanced to force of gravity.

For the quad rotor to yaw to the counter clockwise the opposite operation i.e. the back and front (1st &3rd rotor) shall have speed above the hovering speed factor and that of the left and right (2nd & 4th rotor) shall be decreased from the average/hovering speed.

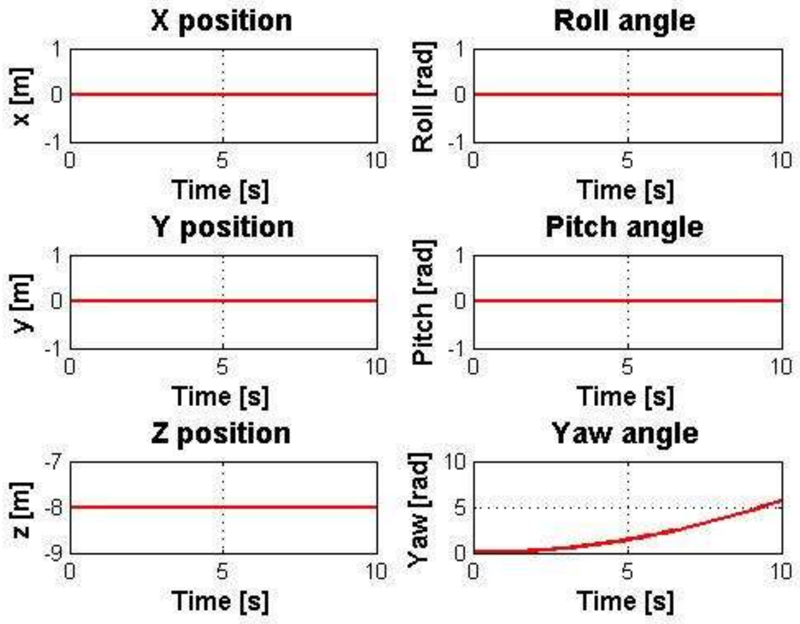

Figure 3-19: Quad-rotor yawing to the clockwiseand hovering still at 8m

When the propeller speed of the left-right rotors is decreased and the front-back is increased the rotorcraft yaws counter clockwise maintaining the vertical thrust in hovering position. In the portrayed scenario we see that the yawing angle is positive i.e. it yaws clockwise direction whereas the opposite scenario would be that the crafts yaws in counter clock wise direction, hence, the angle is negative.

Summarizing this section we have seen the model verification shows that the model adheres to the concept discussed in the principle of operation section and faithfully responds to the control inputs introduced to it. For now the control inputs are the variations of speed of the four rotors.

4 Controller Design and Results

This chapter provides the control law designed to stabilize the quad-rotor at hovering position and the results in regard to the designed controllers.

In the previous section we have seen how the model faithfully responds to the inputs it was commanded with. Here in this section we start designing two control laws that stabilize the craft at hovering position, generally the requirement for control law is for the purpose of controlling the output of processes.

The need for these two control laws is to have a view of the rotorcrafts how fast it responds to the command received and how long it takes to settle to its desired position i.e. hovering. As seen previously in section 3.6 the equilibrium point/hovering position is defined as;

$$\begin{bmatrix} X \\ Y \\ Z \\ \phi \\ \theta \\ \psi \end{bmatrix} = \begin{bmatrix} 0 \\ 0 \\ -8 \\ 0 \\ 0 \\ 0 \end{bmatrix}$$

The next steps after verifying the model are to analyze and design the system to meet the main objective. Using the linearized model in the previous chapter the PID controller and the LQR controller are designed which in turn their performances are evaluated on the dynamics of the linearized model of the vehicle in MATLAB/Simulink.

The controllers gain matrices are found by the linearized model as seen on section 3.5.

4.1 PID Controller

The first controller that was used for stabilizing the craft is the Proportional, Integrator and Derivative (PID) controller. PID is a SISO controller; hence; it only controls the directly actuated DoF i.e. the altitude and attitude (Z, ϕ, θ, and ψ) respectively; whereas the lateral and longitudinal are indirectly actuated, coupled and they cannot be controlled using a SISO controller.

This controller is taken as an extension to the work done by [1]; where in the bench marked paper only the altitude and yaw angle are stabilized using two PID controllers.

There are equal numbers of feedback loops with respect to the directly actuated DoF separated from each other and take the form as shown in the illustration below.

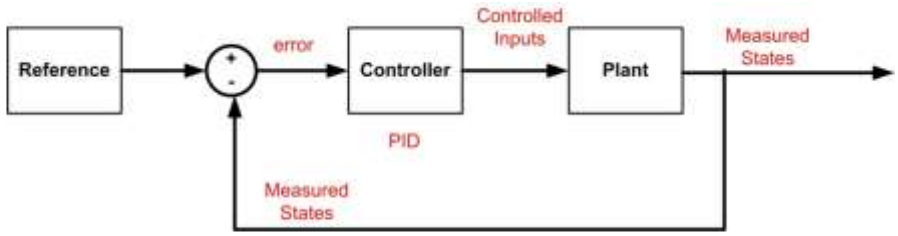

Figure 4-1: PID controller concept implemented in this work

$$U = K_p\, e(t) + K_i \int e(t) + K_d \frac{de}{dt} \qquad \textbf{4-1}$$

Therefore the respective command inputs which stabilize the craft as outputs from the controller are:

$$U_z = K_{pz}\left(Z_{ref} - Z_{actual}\right) + K_{iz} \int (Z_{ref} - Z_{actual}) + K_{dz}\,(\dot{Z}_{ref} - \dot{Z}_{actual})$$

$$U_\phi = K_{p\phi}\left(\phi_{ref} - \phi_{actual}\right) + K_{i\phi} \int (\phi_{ref} - \phi_{actual}) + K_{d\phi}\,(\dot{\phi}_{ref} - \dot{\phi}_{actual}) \qquad \textbf{4-2}$$

(a,b,c,d)

$$U_\theta = K_{p\theta}\left(\theta_{ref} - \theta_{actual}\right) + K_{i\theta} \int (\theta_{ref} - \theta_{actual}) + K_{d\theta}\,(\dot{\theta}_{ref} - \dot{\theta}_{actual})$$

$$U_\psi = K_{p\psi}\left(\psi_{ref} - \psi_{actual}\right) + K_{i\psi} \int (\psi_{ref} - \psi_{actual}) + K_{dz}\,(\dot{\psi}_{ref} - \dot{\psi}_{actual})$$

Using this concept the designed controller was evaluated using MATLAB Simulink; here below the controller block added to the model shown in section 3.6 which was modeled using Simulink model scheme is shown.

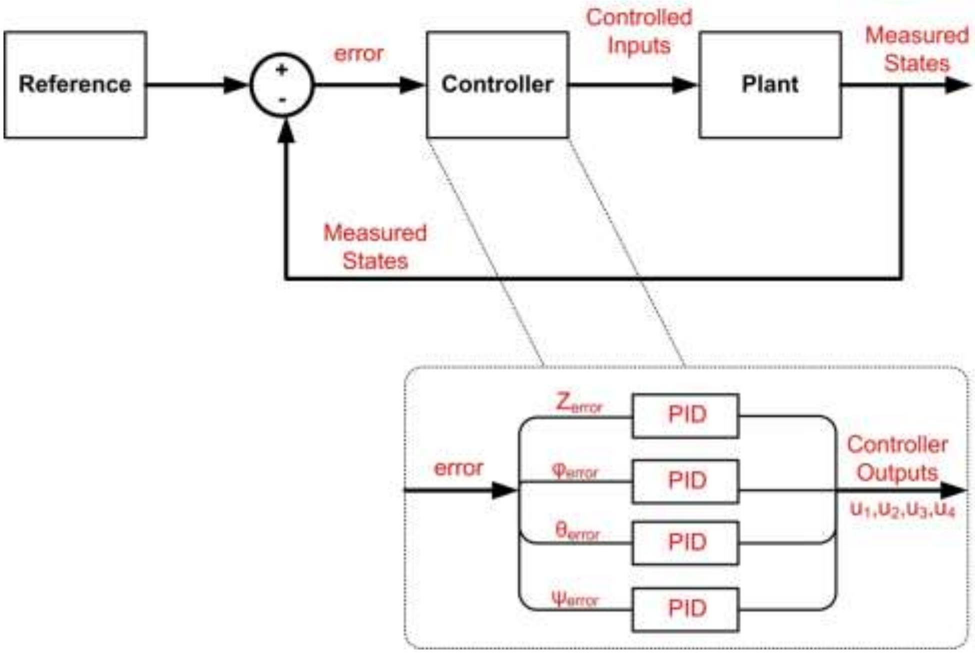

Figure 4-2: PID Controller block

As seen from the figure above we have four independent PID controllers for the actuated states ; with the use of these controllers the craft was stabilized at hovering position but no knowledge its space orientation i.e. know how regarding the longitudinal and latitudinal positions were not acquired. With this result also it is tried to show the controllers capability of stabilizing the craft's altitude and attitude at different points.

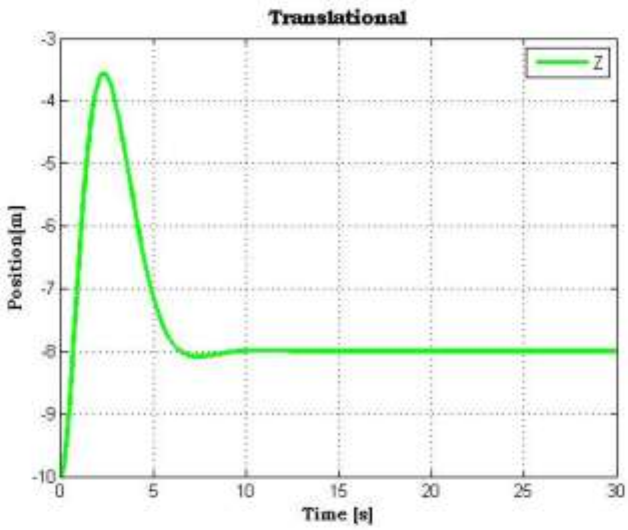

Figure 4-3: Stabilization of Altitude using a PID controller

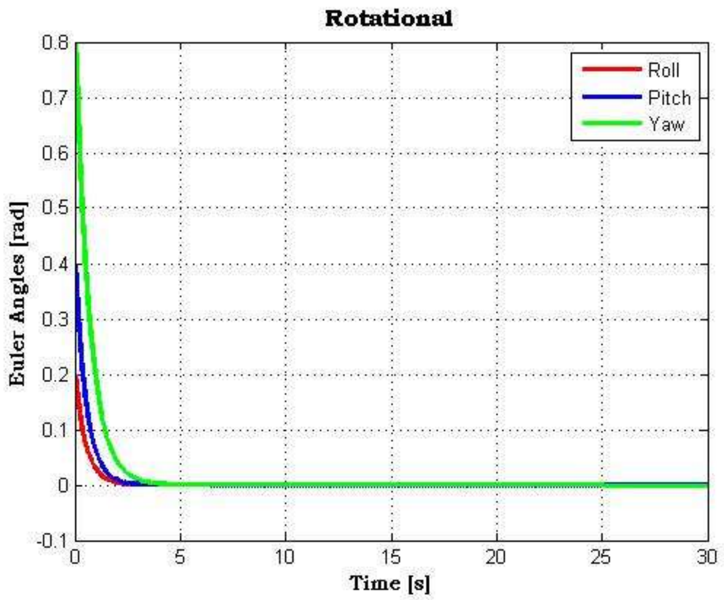

Figure 4-4: Stabilization of Euler Angles using PID controller

The initial states where Z_o=10m, ϕ_o=0.2 rad, θ_o=0.4 rad, ψ_o=0.8 rad and the desired set point the craft was stabilized at its equilibrium point. The altitude takes about 10 seconds to settle whereas the angles were stabilized in less than 5 seconds.

The gain values for the four independent PID controllers were taken from the values of the gain matrix resulted by LQ-servo control by LQR technique (discussed in the following section); whose gain matrix more or less has the structure of a PID controller gain values.

The initial points were chosen on the criteria that the height (altitude) is near to the operating point and for the angles it is preferred that it is kept between the range of +/- 1.57 rad (90˚) for roll and pitch and for yaw about +/- 3.14 (180˚) which in turn also be critical for the coupled translational motions if different from the range.

4.2 LQR Controller

The second controller technique used to design the controller that was used to stabilize the quad-rotor is the linear quadratic regulator. This algorithm uses an optimal control approach i.e. control concerned with operating a dynamic system at minimum cost.

$$J = \int_0^\infty (x'Qx + u'Ru)dt$$

A feedback controller is one of the main results in the theory where the solution is provided by linear quadratic regulator (LQR). Therefore, the effect of this algorithm to find the controller settings that minimizes the undesired deviations from the desired set point (hovering on the equilibrium points regarding to this work).

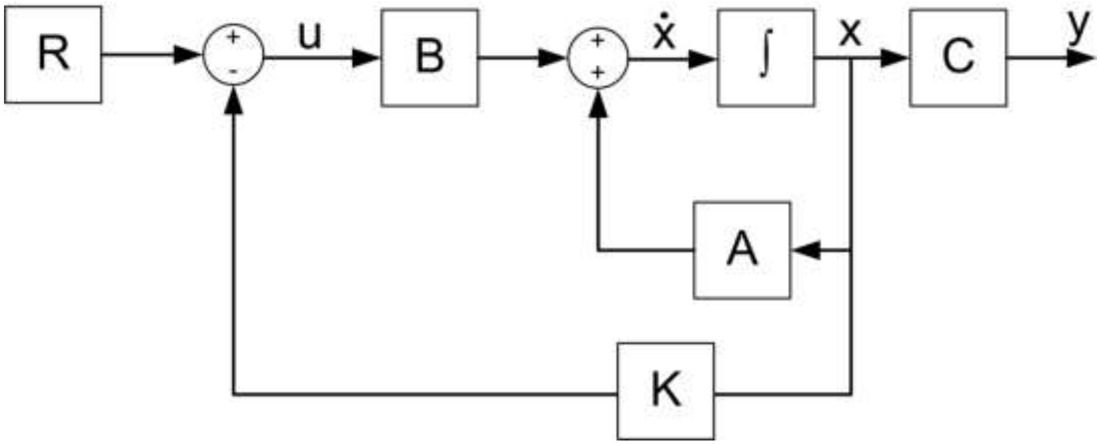

Figure 4-5: State feedback /General LQR (u=-kx)/

The algorithm for LQR at its core is just an automated way of finding an appropriate state feedback controller; with this a much clearer linking between adjusted parameters and the resulting changes in controller behavior is achieved. In this version of the LQR i.e. the state feedback control loop two conditions are held; these are the system is controllable and observable. [30]

4.2.1 Design using Pole Placement

The use of the pole placement technique is to design a state feedback by shifting poles in the real part to the desired places. With this technique a smooth curve without any big overshoots and oscillations can be achieved but guarantee of robustness is in question.

Currently in our design the model has been linearized to its equilibrium point; where the use of pole placement technique is assumed to be the good approach. Values of poles should not be too close to each other and also should not be too far from zero to avoid making the controller hard in terms of the necessary control inputs. By placing the following poles [-1 -1.5 -2 -2.5 -3 -3.5 -4 -4.5 -5 -5.5 -6 -6.5] to our system the following controller gain matrix has been achieved.

$$K = \begin{bmatrix} -4.1723 & -4.8589 & -2.8275 & -2.4480 & -8.5479 & -4.2724 & -6.9141 & -0.6343 & 15.6242 & 1.4864 & 2.7541 & 0.6819 \\ 0.1558 & 0.1465 & 0.5990 & 0.7655 & 0.0057 & 0.0019 & 3.3106 & 0.6004 & -0.4200 & -0.0380 & 0.0131 & 0.0027 \\ -0.2859 & -0.4592 & -0.1507 & -0.1444 & -0.0049 & -0.0005 & -0.4185 & -0.0383 & 2.4068 & 0.5167 & -0.0218 & -0.0059 \\ 0.2075 & 0.2149 & 0.2887 & 0.2581 & -0.0812 & -0.0198 & 0.6914 & 0.0580 & -0.6739 & -0.0666 & 0.2058 & 0.1243 \end{bmatrix}$$

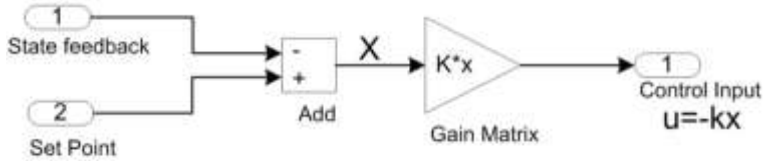

Figure 4-6:LQR controller using pole placement in Simulink

The initial state of the Positions and angles are: X_o = 2 m, Y_o = 3 m, Z_o=10 m; φ_o=0.2 rad, θ_o=-0.4 rad, ψ_o=0.8 rad and the references are equilibrium points (hovering position) respectively.

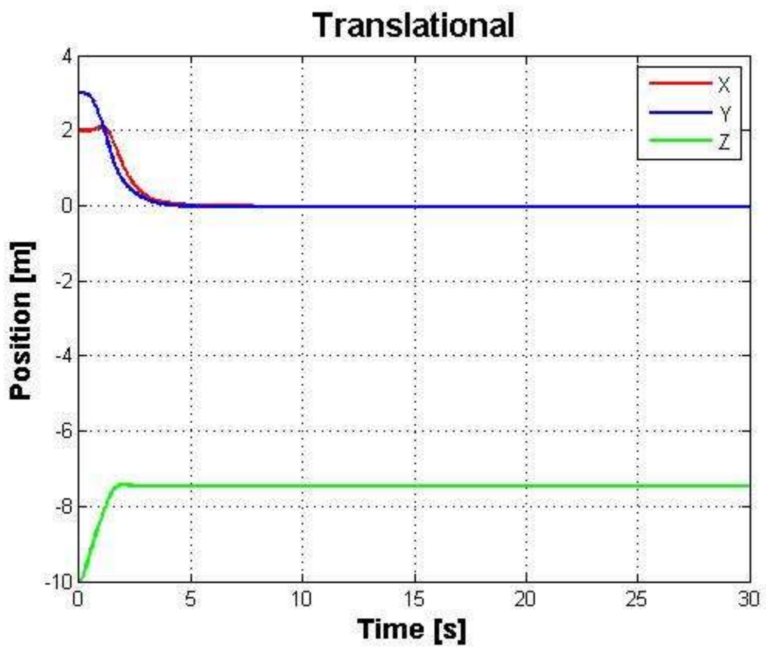

Figure 4-7: Translational motion using pole placement Technique

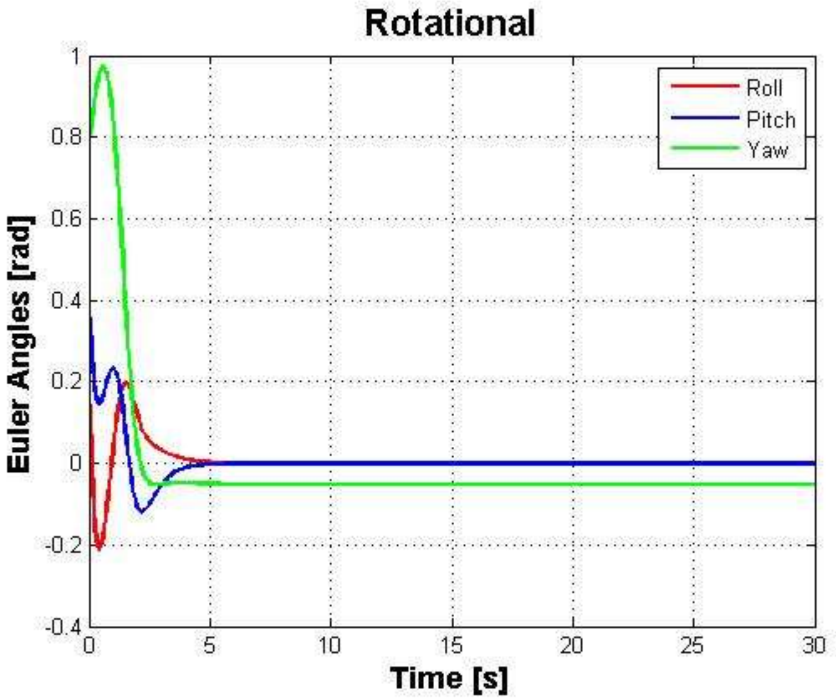

Figure 4-8:Rotational motion using pole placement Technique

It can be seen from Figure 4-7 and Figure 4-8 result that the pole placement technique does not work effectively for all the degrees of freedom; it only stabilizes the X and Y positions and the Roll and Pitch angles towards the desired set point i.e. the hovering position where height and yaw have sustained error from the equilibrium position and orientation respectively.

The lateral and longitudinal positions are stabilized in less than 4 seconds and their corresponding coupled angles settle in less than 5 seconds.

In order to overcome this drawback we introduce the LQ-servo feedback loop to the system in the controller loop to enhance the results using the LQR technique.

4.2.2 Design LQ-Servo feedback using LQR technique

The concept of the LQ-servo feedback is to include the error (the difference between the desired set point of states and the actual state feedbacks) as an extension to the model; hence, the task is to find a feedback that brings the value of the error vector to zero. [31]

The state space model shown earlier can be extended to include the error as shown in the following equations.

$$\dot{x} = Ax + Bu$$

$$y = Cx \qquad \textbf{4-3} \text{ (a,b,c)}$$

$$\dot{x_e} = r - y = r - Cx$$

Therefore, it has the following matrix form

$$\begin{bmatrix} \dot{x} \\ \dot{x_e} \end{bmatrix} = \begin{bmatrix} A & 0 \\ -C & 0 \end{bmatrix} \begin{bmatrix} x \\ e \end{bmatrix} + \begin{bmatrix} B \\ 0 \end{bmatrix} u + \begin{bmatrix} 0 \\ I \end{bmatrix} r \qquad \textbf{4-4}$$

where, x_e represents the error variable taken as states and r the reference set point.

Now that a full state feedback is applied; the value of the feedback gain matrix (K) is calculated as

$$U = -K \begin{pmatrix} x \\ x_e \end{pmatrix}$$

$$K = (K_x \quad K_{xe}) \qquad \textbf{4-5} \text{ (a,b)}$$

For this work K has been designed using the LQR control strategy i.e. solving the algebraic Riccatti Equation (ARE) to minimize the functional cost. The *lqr* command from MATLAB provided the linearized model matrices; has been used to compute the values for K matrix. The K matrix is the horizontal concatenation of the gain from the states and the gain obtained from the error.

$$K_x = \begin{bmatrix} 0 & 0 & 0 & 0 & -0.36 & -0.62 & 0 & 0 & 0 & 0 & 0 & 0 \\ 0 & 0 & 0.27 & 0.29 & 0 & 0 & 1.33 & 0.33 & 0 & 0 & 0 & 0 \\ -0.27 & -0.29 & 0 & 0 & 0 & 0 & 0 & 0 & 1.33 & 0.33 & 0 & 0 \\ 0 & 0 & 0 & 0 & 0 & 0 & 0 & 0 & 0 & 0 & 0.22 & 0.17 \end{bmatrix} \qquad \textbf{4-6} \text{ (a,b)}$$

$$K_{xe} = \begin{bmatrix} 0 & 0 & 0.089 & 0 & 0 & 0 \\ 0 & -0.089 & 0 & 0 & 0 & 0 \\ 0.089 & 0 & 0 & 0 & 0 & 0 \\ 0 & 0 & 0 & 0 & 0 & -0.0894 \end{bmatrix}$$

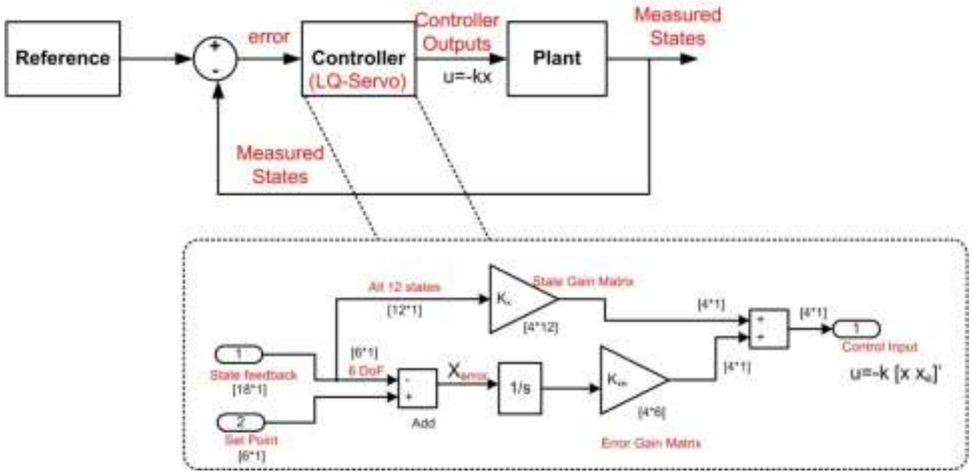

Figure 4-9:LQ-Servo feedback using LQR technique Simulink block

Equipping the original linearized model with additional integrators through this control scheme allows us to follow a constant reference.

The initial state of the Positions and angles are as follows for X_o=2m, Y_o=3m ,Z_o= 10m; φ_o=0.2 rad, θ_o= 0.4 rad, ψ_o=0.8 rad and the references are equilibrium points respectively implying the final position and angles to be stabilized in hovering position.

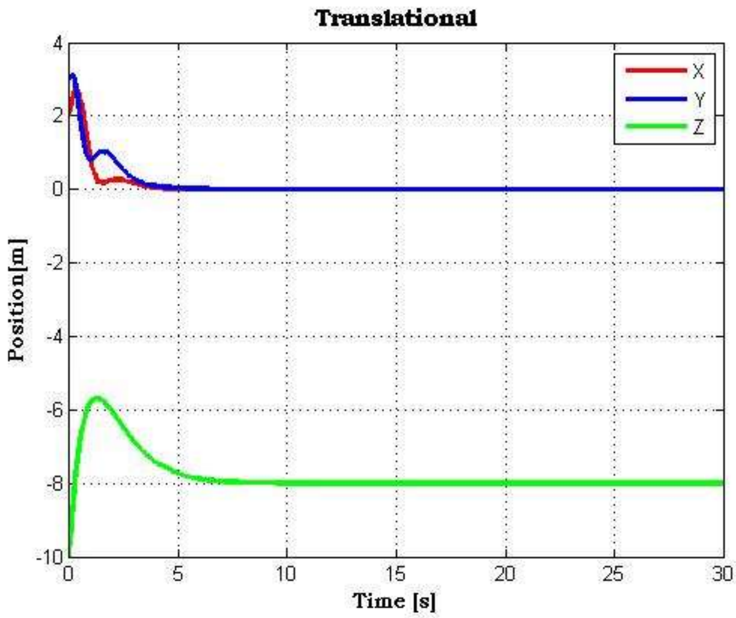

Figure 4-10: Translational motion using LQ-servo feedback technique

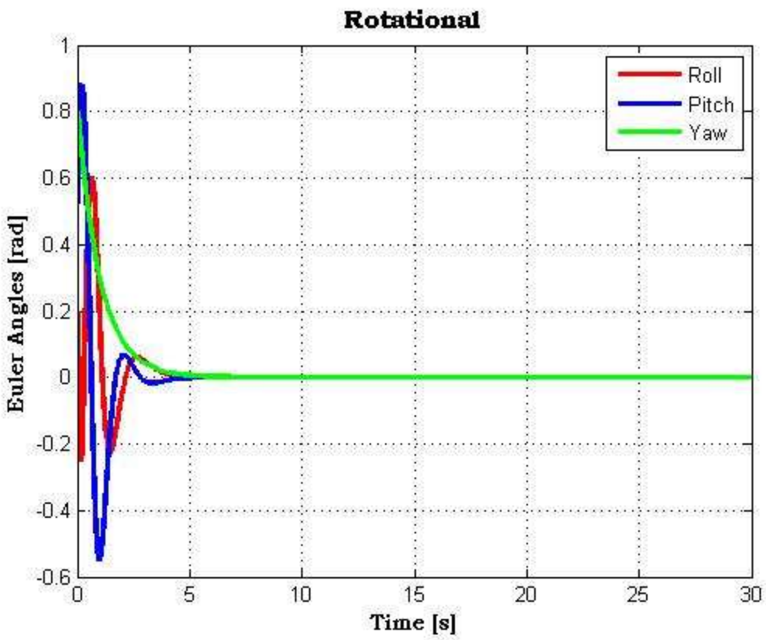

Figure 4-11: Rotational motion using LQ-Servo feedback technique

From the figure illustrated above we can see that the UAV returns back to its hovering position and the controller works effectively and handles the dynamics very well even when the angles were not at the equilibrium point initially. It has stabilized the craft from a different initial translational and angular motion to its equilibrium position (hovering position). The settling time for the X and Y positions is about 4 seconds and for the altitude takes about 9 seconds and for the attitude it takes about 5 seconds.

Using this method has a better settling time for the translational motion but takes a bit longer in order to stabilize the attitude since they are coupled with their respective translational counterparts in comparison to the pole placement method and PID controller.

4.3 Disturbances Introduced

In this section we try to test the performance of the controllers mentioned in the previous sections under the influence of disturbances. Two types of disturbances were introduced to the dynamics of the quad-rotor.

Scenario I: Wind disturbance

The first type of disturbance that was introduced to the modeled system is some force that pulls/drags the craft to different positions, angles. The disturbance is introduced to both the translational and rotational motions.

This disturbance is introduced in the model using the step input block from Simulink initially in a different point to a craft that is hovering at its equilibrium point and in turn using the controllers to stabilize it to the initial hovering position.

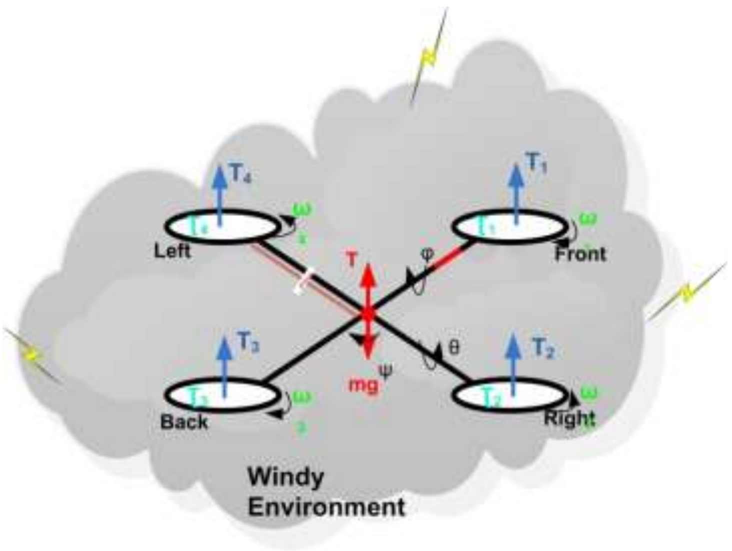

Figure 4-12:Conceptual Diagram showing the craft in a windy environment

In Figure 4-13 the disturbance introduced to the model is illustrated using Simulink modeling blocks.

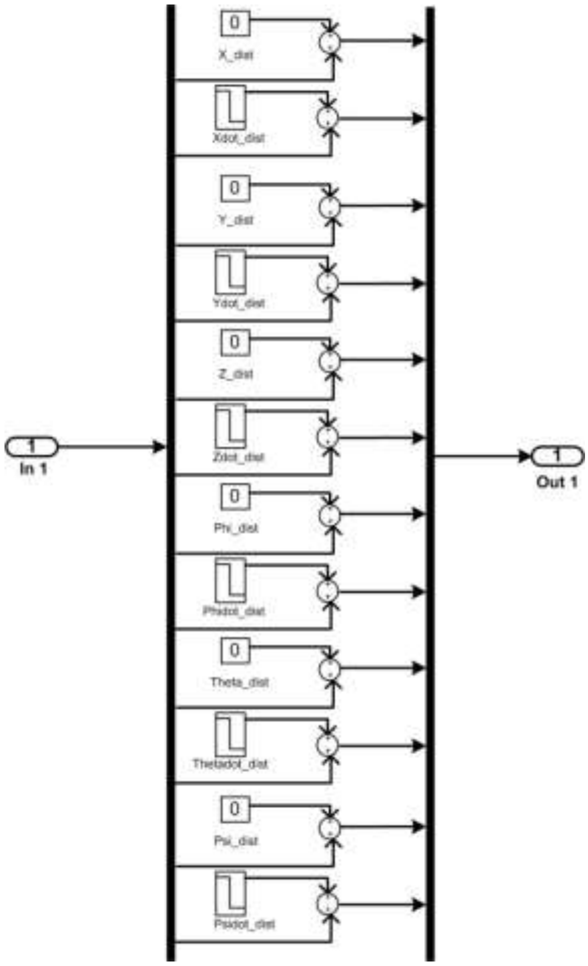

Figure 4-13: Disturbance model

This disturbance is added to the states i.e. the translational and rotational velocities and fed back again to the dynamics. Using the control inputs from the controller; it tries to stabilize the craft under the influence of disturbance that would pull/drag it. With this disturbance it is assumed that an external environment disturbance such as wind disturbs the quad-rotor's motion in undesirable directions.

To simulate the disturbance a step input is introduced to each velocity of the states. Here below the results are discussed.

These disturbances are introduced to the altitude and attitude that can be stabilized by using a PID controller.

$$\begin{bmatrix} Z_{dist} \\ \phi_{dist} \\ \theta_{dist} \\ \psi_{dist} \end{bmatrix} = \begin{bmatrix} \dot{Z} + 2 \\ \dot{\phi} + 0.4 \\ \dot{\theta} + 0.6 \\ \dot{\psi} + 0.8 \end{bmatrix}$$

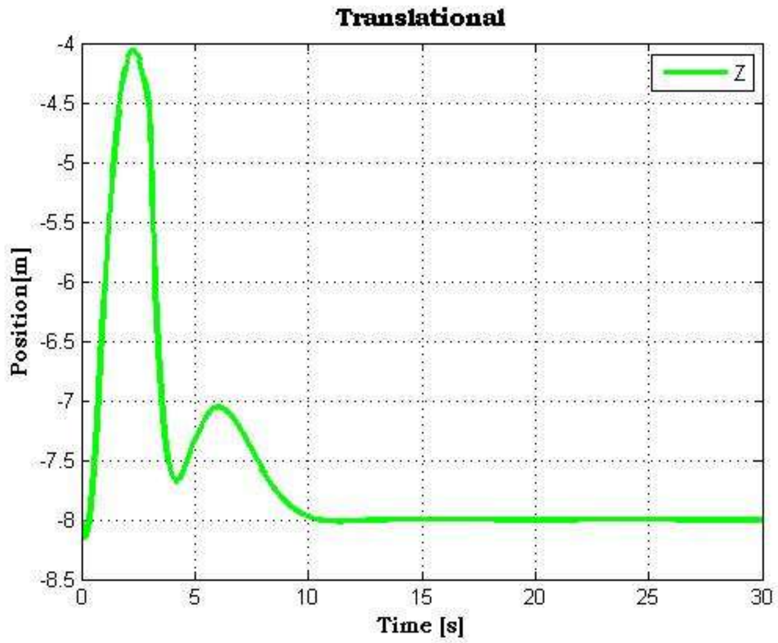

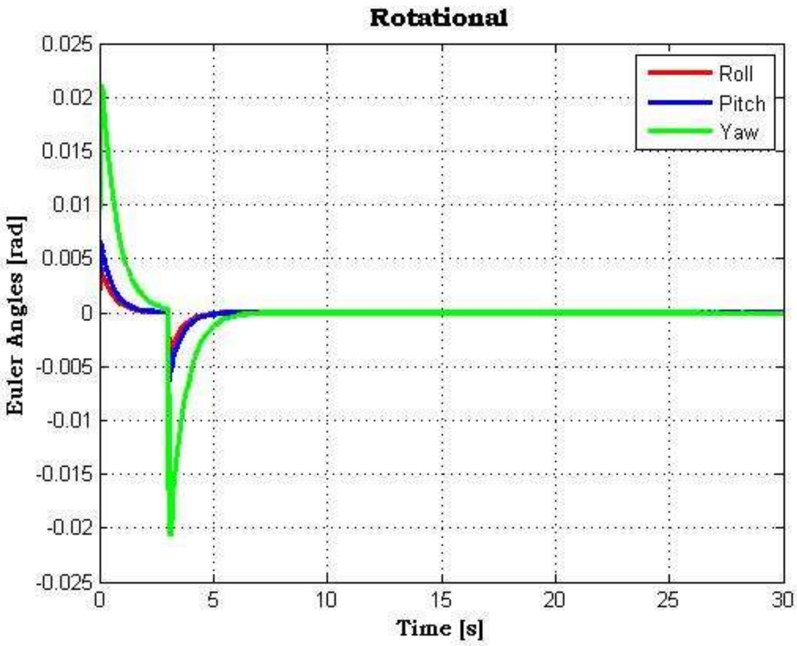

Figure 4-14: Altitude and Attitude Stabilization with disturbance using PID controller

From the above plotted results it is shown that the disturbance introduced here is the assumed windy environment where the disturbance is added to each state velocity of the craft. With the introduction of disturbance it can be seen that the altitude of the craft loses its altitude not only because disturbance was introduced to it directly but also because of the imbalance created when the angles are disoriented due to the addition of disturbance; this is supported by the concept discussed on principle of operation under the scenario of roll and pitch. The controller stabilizes the DoF back to their initial hovering position within 7 seconds for the attitude whereas the altitude takes about 11 seconds to settle.

Disturbances introduced to all states that can be stabilized by the LQR controller as shown below; here the lateral and longitudinal positions are included to the disturbance mentioned earlier.

$$\begin{bmatrix} X_{dist} \\ Y_{dist} \\ Z_{dist} \\ \phi_{dist} \\ \theta_{dist} \\ \psi_{dist} \end{bmatrix} = \begin{bmatrix} \dot{X} + 2 \\ \dot{Y} + 3 \\ \dot{Z} + 2 \\ \dot{\phi} + 0.4 \\ \dot{\theta} + 0.6 \\ \dot{\psi} + 0.8 \end{bmatrix}$$

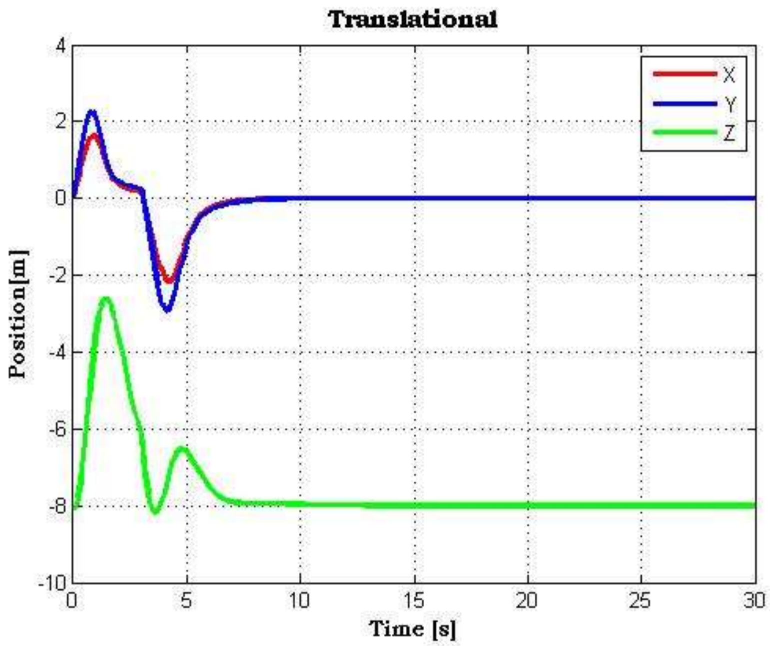

Figure 4-15:Position stabilization after disturbance using LQR controller

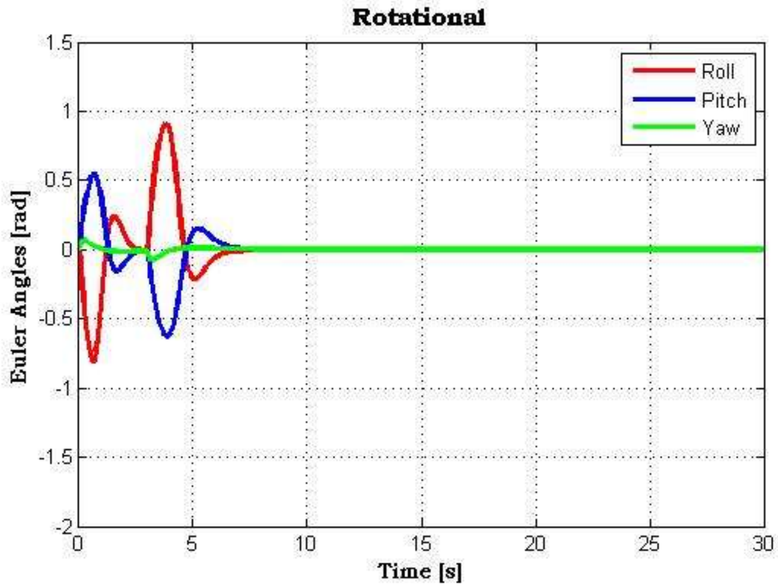

Figure 4-16: Attitude Stabilization with disturbance using LQR controller

From the results depicted we see the concept discussed under the topic of the principle of operation is also supported here. We see that due to the disturbance in the translational motion there is an effect in its respective coupled rotational motion while accommodating the disturbance introduced to it and vice versa. The LQR controller takes more time to settle than the PID controller because in this scenario the lateral and longitudinal DoF are also taken into consideration. The LQR controller takes about 9 seconds to settle the roll and pitch angle while the yaw angle settles in 5 seconds. Moreover the translational motion settles in about 8 seconds for the X and Y positions while the altitude takes 12 seconds to settle.

The reason why the altitude takes a longer time to settle using LQR controller is that before the altitude gets stabilized the controller tries to stabilize the other coupled degrees of freedom; hence while trying to accommodate the disturbance added to the roll angle the Y position gets disturbed which in turn creates instability in the altitude. The yaw angle settles faster than any other DoF because it is not coupled to any of the other states.

Scenario II: Side Jerk

The second disturbance that is introduced to the model is some jerk that makes an impact to the craft. It has been only introduced to one of the states i.e. X-position to have a side drift initially from its equilibrium hovering position. However, for this scenario with which PID controller is going to be used a jerk force to the acceleration in the Z-position has been introduced since this controller is only capable to control the directly actuated DoF.

This disturbance is included in the model using a gain block from Simulink to be multiplied to the direct output of the dynamics i.e. the state derivatives. Therefore, the gain is multiplied to the acceleration in the X-direction and Z-axis for the respective type of control algorithm to be used.

For the LQR control algorithm, the jerk motion moves the craft sideways with its coupled angle (i.e. the pitch angle) being disoriented to some undesirable position and it is tried to revive it to get back to the desired hovering position; while for the PID control algorithm the jerk in the Z-position makes the craft lose its balance in holding its altitude but then again it has been stabilized to its initial hovering position and has no effect on the attitude.

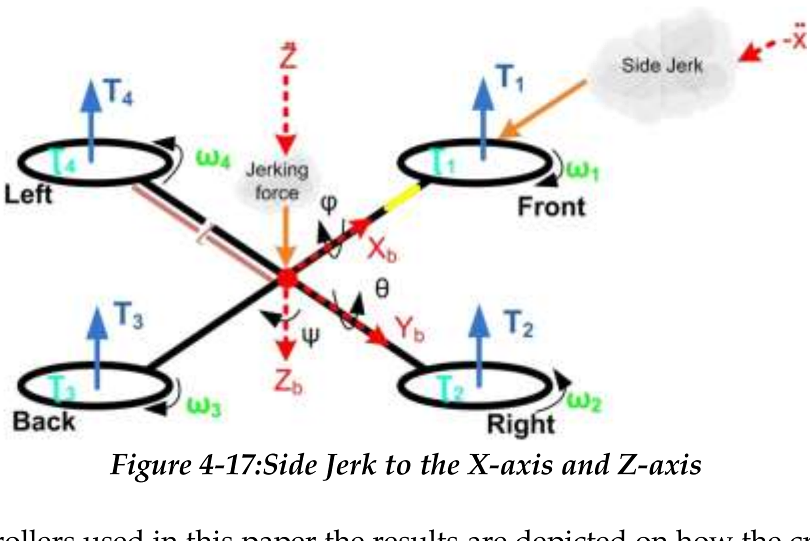

Figure 4-17:Side Jerk to the X-axis and Z-axis

Using the controllers used in this paper the results are depicted on how the craft stabilizes to its initial position. In Figure 4-18 a Simulink modeling figure is shown to illustrate the concept on how the disturbance is included to the model.

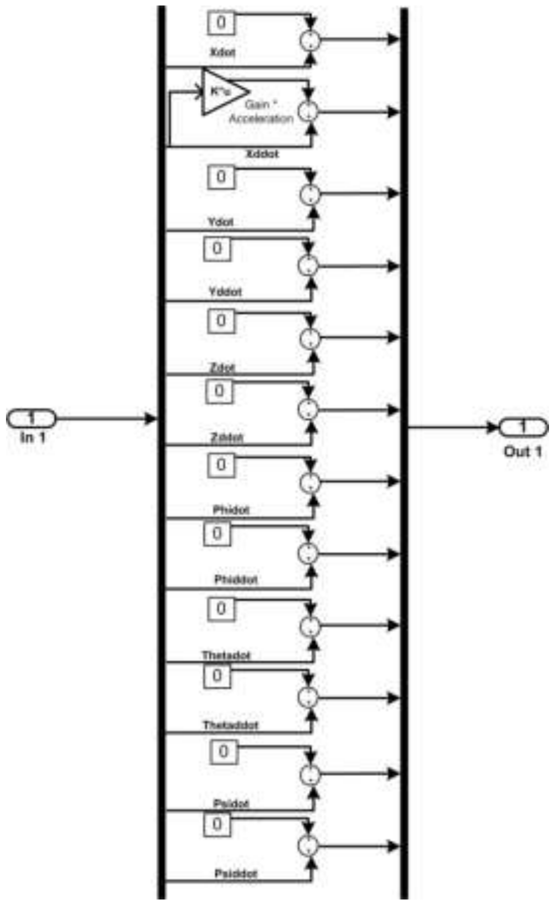

Figure 4-18:Side Jerk Disturbance model

This disturbance is added to the one of the state derivatives; the result of the dynamics. The Side drift moves the quad-rotor to the direction it was applied i.e. the –x direction as shown on the conceptual diagram on Figure 4-17.

In Figure 4-19 the result for the stabilization of the craft after a jerk has been introduced to the altitude is shown.

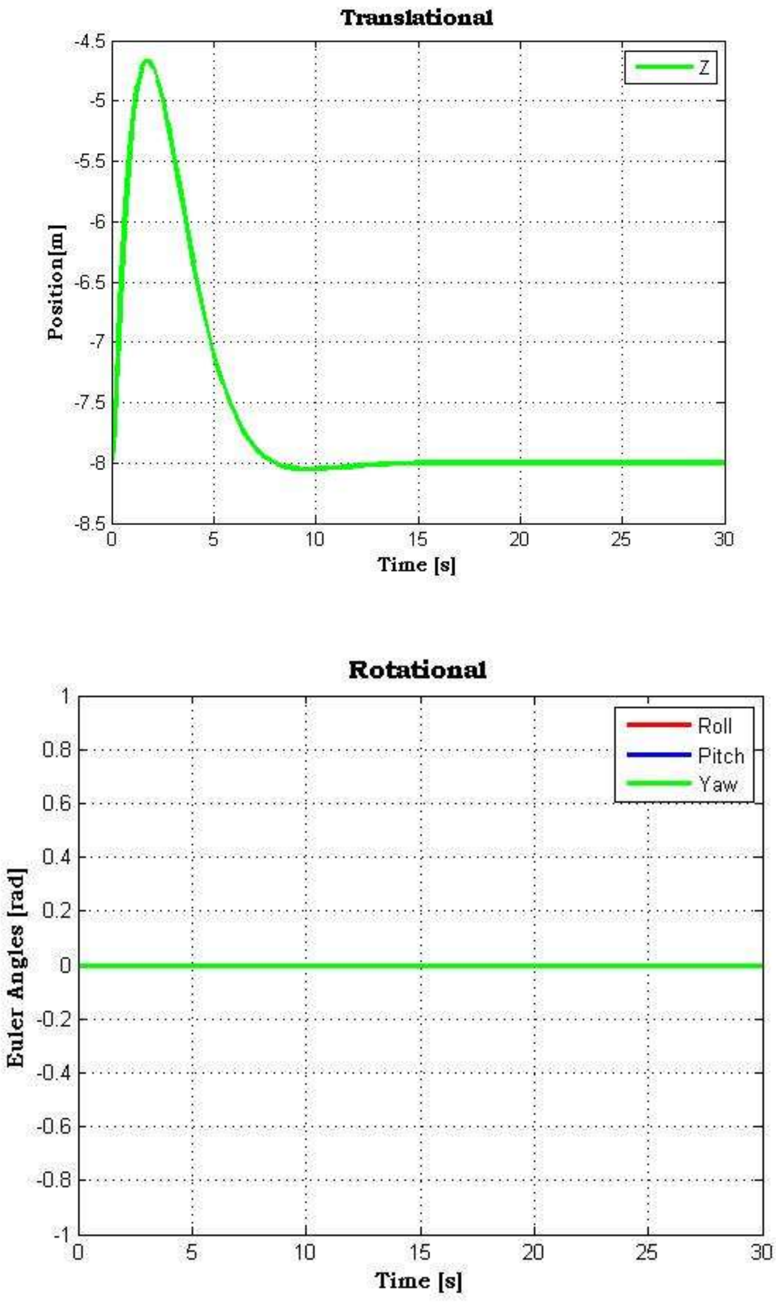

Figure 4-19:Altitude and Attitude Stabilization with Jerking force to the Z-axis using PID controller

Using the PID controller the craft was stabilized to hovering position after the introduction of a jerking disturbance to its vertical acceleration at the Z-axis. The jerk drives the craft to move below the hovering position from 8m height to about 4m height and settles back to its initial hovering position at about 10 seconds. Since the altitude is not coupled with any of the other DoF the angles are not affected by the introduction of jerking disturbance to the altitude. The angles are still in their hovering position even though the altitude was disturbed and stabilized back.

In Figure 4-21 and Figure 4-21 the results for the stabilization of the craft after a jerk has been introduced to the X-axis are shown. Definitely, the coupled angle will also be destabilized for some time before both the lateral motion and its coupled pitch angle get stabilized back to its initial hovering position.

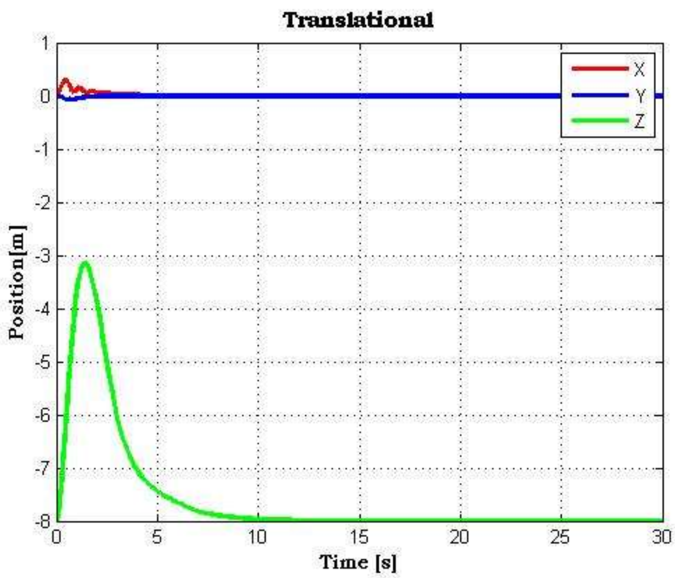

Figure 4-20: Position Stabilization with Side jerk to the X-axis using LQR controller

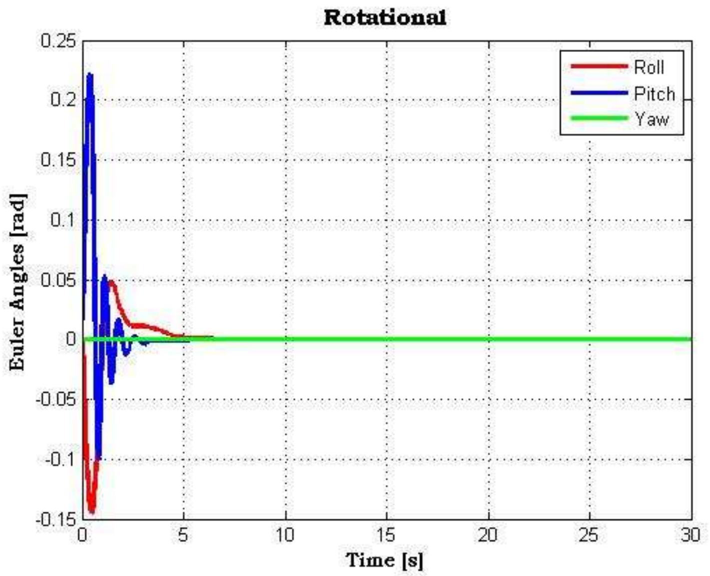

Figure 4-21: Attitude Stabilization with Side jerk to the X-axis using LQR controller

By introducing a side jerk to the X-axis it is evident that there will be instability in the altitude and that the respective coupled angle will be disoriented. In the results illustrated the concept discussed in the above line has been shown clearly. The lateral position is disturbed for about 5 seconds but its coupled angle (pitch) is stabilized due to the side jerk in 4 seconds.

Due to the imbalance in the lateral position and the coupled angle, the altitude loses its balance of holding the craft in its hovering position. In about 11 seconds the altitude is stabilized after settling the angle to its desired hovering position. The longitudinal position and the roll angle are also disturbed in the process of stabilizing the lateral position and the pitch angle and these are stabilized in about 2 seconds and 5 seconds respectively. The yaw is insignificantly disturbed as it is not coupled with any of the other degrees of freedom and stays at its desired position.

Summarizing this section based on the results looked over in the previous sections; we see that the use of the LQR technique for the scheme of controlling the craft to stabilize in its hovering position involves all 6 DoF and takes a bit longer than the PID controller, which is a classical SISO controller that only considers the directly actuated degrees of freedom.

5 Conclusions and Recommendations

5.1 Contribution

This thesis started with the recommendation from [1] which is stated as one of the points on the statement of the problem. In the paper [1] stabilization of the yaw and altitude was carried out; in this thesis an enhancement has been made by including the rest of the attitude and used PID and LQR controller to stabilize the quad-rotor in the desired position i.e. hovering position by taking all the states that define the dynamics.

5.2 Conclusion

In this thesis general history about unmanned aerial vehicles with specifics about quad-rotor has been discussed and no matter what their configuration is their characteristics are merely similar i.e. all UAVs are under actuated, coupled and have 6 DoF.

The Newton-Euler formulation has been used as the modeling method from many others as it is a comprehensible modeling method. Nonlinear dynamics has been formulated based on the understanding of the operation and the works by [19]

Once the model had been formulated it was linearized to an equilibrium point where the hovering position has been defined to be; then it was sought out to verify the model if it responds to the inputs that it was commanded to and whether the dynamics and operations discussed in section 3.5 are seen with this model of the craft. The model verification was successful and it has been seen that the modeled dynamics faithfully responds to the commanded inputs.

Right after the verification of the model; the starting point was to extend the work of [1] i.e. to include the rest of the other Euler angles that make up the attitude of the rotorcraft and stabilize the altitude together with the attitude with a SISO classical controller (PID). With this controller the directly actuated degrees of freedom have been stabilized.

The next step was to introduce a controller that considers all degrees of freedom to be controlled. Hence, an optimal controller that minimizes the cost (error) and outputs an input that could bring the optimized output i.e. linear quadratic regulator (LQR) was introduced. The controller feedback gain matrix has been found from the linearized model. With the two controllers, the stabilization of the quad-rotor at hovering position was successful.

Finally two different disturbances were introduced to explore more about the controllers if they adhere to the desired response i.e. stabilizing the craft back to hovering position even though there would be some external environmental factors prohibiting it. A wind disturbance and a side jerk introduced that moves the UAV in different directions is stabilized.

Generally summarizing the work done here in this paper is:

- extended the work of [1] by stabilizing the altitude and attitude;
- modeled and simulated using MATLAB and SIMULINK;
- stabilizing the quad-rotor at hovering position; all the 6 DoF and
- Inclusion of external environmental factors and stabilizing it back to its equilibrium point/hovering position.

5.3 *Future Works*

Although this thesis has successfully accomplished the mission which was targeted; not all things have been done and there other different issues and works to be done with in this subject.

Recommendations for future work from this work are listed down below:

- Input optimization to controlled motors
- Model and control the craft for non-hovering operation
- Include other effects such as rolling moments, ground effect and hub forces to the model
- Introduce nonlinear controllers and new controllers that would make the stabilization of the craft in the desired operation effective
- Consideration of flapping and tilting of blades
- Model of combat operation could also be included
- Stabilization of crafts during a formation flight
- Communication with remote operation rooms during a reconnaissance mission could be included if considered for military operation
- Last but not least, integration of the characteristics in an electronic warfare environment could be useful for tactical and counter measure operations.

6 References

1. **A.Ouladi.** *Four Rotors Helicopter Yaw and Altitude Stabilization.* Algeria : Control and Command laboratory EMP, 2007.

2. **Lee, Keun Uk.** *Modeling and Altitude Control of quadrotor UAV.* Seoul,South Korea : Department of Electrical and Electronics Engineering, Yonsei University, 2011.

3. **Syed Ali Raza, Wail Gueaieb.** *Intelligent Flight Control of an Autonomous Quadrotor.* Canada : University of Ottawa, 2009.

4. **Venditelli, Marilena.** *Quadrotor Modeling.* Rome : Sapienza,University di Roma, 2011.

5. **Meric, Hugo.** *Stabilization of Four rotors UAV.* Australia : Institut Superieur de l'Aeronautique et de l'Espace and National ICT Australia, 2010.

6. **K.J.Yoon.** *Design of an Autonomous Hover Control System for a Samll Quadrotor.* South Korea : Konkuk University,Aerospace Information Engineering Department, 2010.

7. **Samir Bouabdallah, Andre Noth,Ronald Siegwart.** *PID vs LQ Control Techniques Applied to an Indoor Micro Quadrotor.* Lausanne,Switzerland : Autonomous Systems Laboratory, Swiss Federal Institute of Technology, 2004.

8. **Birkan Tunç, K. Oytun Yapıcı.** *Fuzzy Logic Control of a Four Rotor Unmanned Air Vehicle.* 2006.

9. **M.Raju Hossain, D.Geoff Rideout,D.Nicholas Krouglicof.** *Bond Graph Dynamic Modeling and Stabilization of a Quadrotor helicopter.* Newfoundland,Canada : University of Newfoundland, 2008.

10. **Bresciani, Tommaso.** *Modeling, Identification and Control of a Quadrotor Helicopter.* Sweden,Lund University : Department of Automatic Control, 2008.

11. Draganfly website. [Online] http://www.draganfly.com.

12. **J.G.Leishman.** *Principles of Helicopter Aerodynamics.* Maryland : Cambridge University Press, 2000.

13. Century-of-Flight. [Online] http://www.Century-of-Flight.com.

14. **J.G.Leishman.** *The Breguet-Richet Quadrotor Helicopter of 1907.* Maryland : University of Maryland, 2001.

15. Unmanned Aerial Vehicle Systems Association. [Online] http://www.uavs.org.

16. Ascending Technologies. *Humming Bird Quadrotor UAV.* [Online] http://www.asctec.de.

17. **Miller, Katie.** *Path Tracking Control for Quadrotor Helicopters.* 2008.

18. **C.Nicol, C.J.B Macnab,A.Ramirez-Serrano.** *Robust Neural Network of a Quadrotor Helicopter.* Calgary and Alberta,Canada : IEEE, 2008.

19. **Samir Bouabdallah, Ronald Siegwart.** *Design and Control of a Miniature Quadrotor.* ETH Zurich,Switzerland : Autonomous Systems Lab, 2007.

20. **Paul Pounds, Robert Mahony ,Peter Corke.** *Modelling and Control of a Quadrotor Robot.* Canberra and Brisbane, Australia : CSIRO ICT Centre,Australian National University, 2010.

21. **Y.Naidoo.** *Quadrotor Unmanned Aerial vehicle Helicopter Modeling and Control.* South Africa : University of KwaZulu-Natal, 2011.

22. **Topalov, Andon Venelinov.** *Comparative Results on Stabilization of the Quad-rotor Rotorcraft Using Bounded Feedback Controllers.* s.l. : Springer Science+Business Media, 2011.

23. **Inge Troch, Felix Breitenecker.** *Modeling and Simulation of Dynamic Systems.* Vienna,Austria : University of Technology, 2007.

24. **Bak, Thomas.** *Modeling of Mechanical Systems.* Aalborg,Denmark : Department of Control Engineering,Aalborg, 2002.

25. **Schmidt, Michael David.** *Simulation and Control of a Quadrotor Unmanned Aerial vehicle.* s.l. : University of Kentucky, 2011.

26. **Administration, Federal Aviation.** *Rotorcraft Flying Handbook.* s.l. : U.S. Department of Transportation. FAA-H-8083-21.

27. **Yenehun, Abeje.** *Model and Robust Control of an Unmanned Aerial vehicle* . Enschede : University of Twente, 2011.

28. **Latorre, Eva Saddre.** *Propulsion system optimization for an unmanned lightweight quadrotor.* s.l. : Universitat Politècnica de Catalunya, 2011.

29. **Bramwell, Robert.** *Principles of Helicopter Flight.* 1992.

30. **Hespanha, Joao P.** *LQG/LQR Controller Design.* Santa Barbara : University of California, April 2007.

31. *Feedback Control Systems.* Massachusetts : Massachusetts Institute of Technology, 2010.

Appendix

A. Rotation Matrix

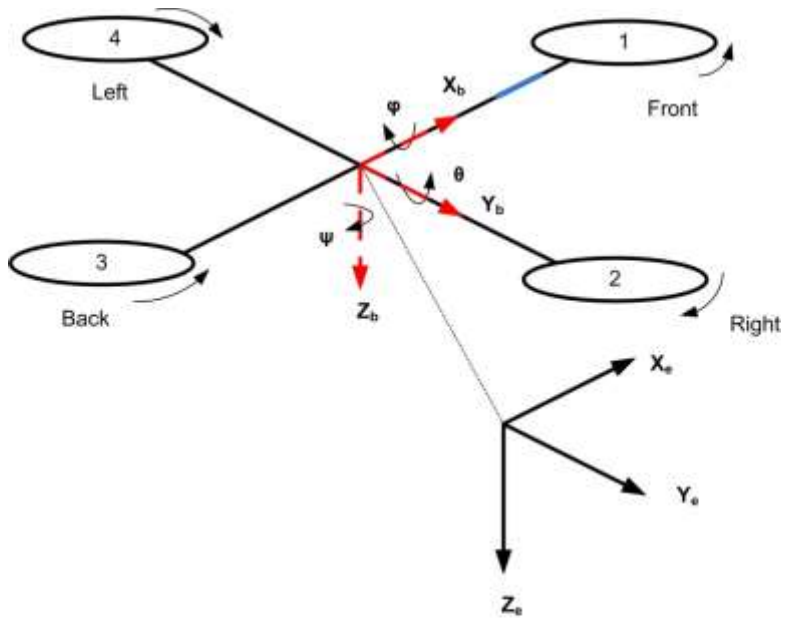

Figure Appendix-A 1: Relation of the Inertial Frame (IF) with body Fixed Frame (BFF)

The linear position is determined by the coordinates of the vector between the origin of the BFF and that of the IF with respect to the Inertial frame; whereas the angular position is defined by the orientation of the BFF with respect to the IF.

The attitude i.e. angular position in respect to the IF is determined by three successive rotations about the main axes which take IF into BFF.

By multiplying the three basic rotation matrices in a 1-2-3 sequence i.e. first the rotation about the z-axis, then about the y-axis and finally about the x-axis. The three successive rotations are shown next:

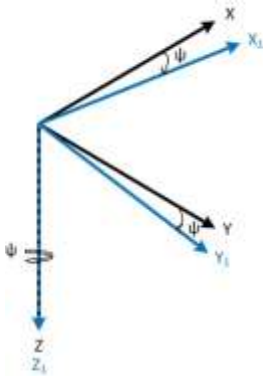

$$R_{\psi} = \begin{bmatrix} C_{\psi} & -S_{\psi} & 0 \\ S_{\psi} & C_{\psi} & 0 \\ 0 & 0 & 1 \end{bmatrix}$$

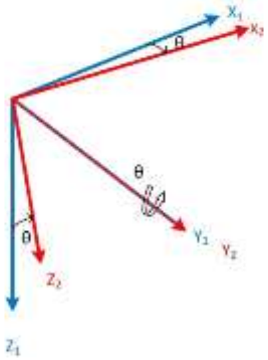

$$R_{\theta} = \begin{bmatrix} C_{\theta} & 0 & S_{\theta} \\ 0 & 1 & 0 \\ -S_{\theta} & 0 & C_{\theta} \end{bmatrix}$$

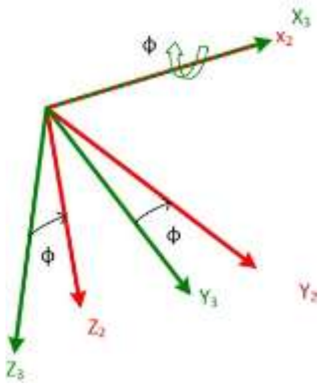

$$R_{\phi} = \begin{bmatrix} 1 & 0 & 0 \\ 0 & C_{\phi} & -S_{\phi} \\ 0 & S_{\phi} & C_{\phi} \end{bmatrix}$$

The notations $C_t$and S_t indicate Cos t and Sin t respectively.

Hence, the transformation which relates the motions of Body fixed frame with respect to the inertial frame is construed as follows:

$$R = R_{\psi} R_{\theta} R_{\phi}$$

$$R = \begin{bmatrix} C_\psi C_\theta & C_\psi S_\theta S_\phi - S_\psi C_\phi & C_\phi S_\theta C_\psi + S_\phi S_\psi \\ S_\psi C_\theta & S_\psi S_\theta S_\phi + C_\psi C_\phi & C_\phi S_\theta S_\psi - S_\phi C_\psi \\ -S_\theta & C_\theta S_\phi & C_\phi C_\theta \end{bmatrix}$$

B. Transfer Matrix

$$\begin{bmatrix} \dot\phi \\ \dot\theta \\ \dot\psi \end{bmatrix}_I = \begin{bmatrix} \dot\phi \\ 0 \\ 0 \end{bmatrix} + R_\phi^{-1} \begin{bmatrix} 0 \\ \dot\theta \\ 0 \end{bmatrix} + R_\phi^{-1} R_\theta^{-1} \begin{bmatrix} 0 \\ 0 \\ \dot\psi \end{bmatrix} = T \begin{bmatrix} \dot\phi \\ \dot\theta \\ \dot\psi \end{bmatrix}_B$$

$$\begin{bmatrix} \dot\phi \\ \dot\theta \\ \dot\psi \end{bmatrix}_I = \begin{bmatrix} \dot\phi_B \\ 0 \\ 0 \end{bmatrix} + \begin{bmatrix} 1 & 0 & 0 \\ 0 & C_\phi & S_\phi \\ 0 & -S_\phi & C_\phi \end{bmatrix} \begin{bmatrix} 0 \\ \dot\theta_B \\ 0 \end{bmatrix} + \begin{bmatrix} 1 & 0 & 0 \\ 0 & C_\phi & S_\phi \\ 0 & -S_\phi & C_\phi \end{bmatrix} \begin{bmatrix} C_\theta & 0 & -S_\theta \\ 0 & 1 & 0 \\ S_\theta & 0 & C_\theta \end{bmatrix} \begin{bmatrix} 0 \\ 0 \\ \dot\psi_B \end{bmatrix} = T \begin{bmatrix} \dot\phi \\ \dot\theta \\ \dot\psi \end{bmatrix}_B$$

$$\begin{bmatrix} \dot\phi \\ \dot\theta \\ \dot\psi \end{bmatrix}_I = \begin{bmatrix} \dot\phi_B \\ 0 \\ 0 \end{bmatrix} + \begin{bmatrix} 1 & C_\phi & -S_\phi \end{bmatrix} \begin{bmatrix} 0 \\ \dot\theta_B \\ 0 \end{bmatrix} + \begin{bmatrix} C_\theta & 0 & -S_\theta \\ S_\phi S_\theta & C_\phi & S_\phi C_\theta \\ C_\phi S_\theta & -S_\phi & C_\phi C_\theta \end{bmatrix} \begin{bmatrix} 0 \\ 0 \\ \dot\psi_B \end{bmatrix} = T \begin{bmatrix} \dot\phi \\ \dot\theta \\ \dot\psi \end{bmatrix}_B$$

$$\begin{bmatrix} \dot\phi \\ \dot\theta \\ \dot\psi \end{bmatrix}_I = \begin{bmatrix} \dot\phi_B \\ 0 \\ 0 \end{bmatrix} + \begin{bmatrix} 1 & C_\phi & -S_\phi \end{bmatrix} \begin{bmatrix} 0 \\ \dot\theta_B \\ 0 \end{bmatrix} + \begin{bmatrix} -S_\theta & S_\phi C_\theta & C_\phi C_\theta \end{bmatrix} \begin{bmatrix} 0 \\ 0 \\ \dot\psi_B \end{bmatrix} = T \begin{bmatrix} \dot\phi \\ \dot\theta \\ \dot\psi \end{bmatrix}_B$$

$$\begin{bmatrix} \dot\phi \\ \dot\theta \\ \dot\psi \end{bmatrix}_I = T \begin{bmatrix} \dot\phi \\ \dot\theta \\ \dot\psi \end{bmatrix}_B$$

$$\begin{bmatrix} \dot\phi \\ \dot\theta \\ \dot\psi \end{bmatrix}_I = \begin{bmatrix} 1 & 0 & -S_\theta \\ 0 & C_\phi & S_\phi C_\theta \\ 0 & -S_\phi & C_\phi C_\theta \end{bmatrix} \begin{bmatrix} \dot\phi \\ \dot\theta \\ \dot\psi \end{bmatrix}_B$$

With the transfer matrix gained from the above calculation and the operating point gained in section 3.5.2; we see that the transfer matrix that is used to relate the angular velocity from the inertial frame to the body frame is an Identity matrix for hovering flight regime.

At hovering position the attitude angles are at zero i.e. $\phi=0$, $\theta=0$, $\psi=0$; hence the transfer matrix is shown below

$$\begin{bmatrix} \dot\phi \\ \dot\theta \\ \dot\psi \end{bmatrix}_I = \begin{bmatrix} 1 & 0 & 0 \\ 0 & 1 & 0 \\ 0 & 0 & 1 \end{bmatrix} \begin{bmatrix} \dot\phi \\ \dot\theta \\ \dot\psi \end{bmatrix}_B$$

With the above shown equation we see that the angular velocity in the inertial frame and the angular velocity in the body frame is the same for hovering flight.

C. Parameters of DraganFlyer IV

The parameters that were used for simulation were adopted from the literature by A.Ouladi and they are listed below

- Mass (m) =500 g
- Gravity (g) =9.81 m/s2
- Length of the arm between the CoG and the tip where rotor is placed (l)= 22.5 cm
- Thrust Coefficient (b) = 3.13x10-5 N/rad/s
- Drag Coefficient (d) = 9x10-7 N.m/rad/s
- Inertia Matrix (Ixx,Iyy,Izz) = $\begin{bmatrix} 0.0086 & 0 & 0 \\ 0 & 0.0086 & 0 \\ 0 & 0 & 0.0172 \end{bmatrix}$ N.m/rad/s2

D. Details on Linearization